# Genomic analysis of European *Drosophila* populations reveals major longitudinal structure, continent-wide selection, and unknown DNA viruses

Martin Kapun[1,2,3,4,†,*], Maite G. Barrón[1,5,*], Fabian Staubach[1,6,§], Jorge Vieira[1,7,8], Darren J. Obbard[1,9], Clément Goubert[1,10,11], Omar Rota-Stabelli[1,12], Maaria Kankare[1,13,§], María Bogaerts-Márquez[1,5], Annabelle Haudry[1,10], R. Axel W. Wiberg[1,14,15], Lena Waidele[1,6], Iryna Kozeretska[1,16,17,], Elena G. Pasyukova[1,18], Volker Loeschcke[1,19], Marta Pascual[1,20], Cristina P. Vieira[1,7,8], Svitlana Serga[1,16], Catherine Montchamp-Moreau[1,21], Jessica Abbott[1,22], Patricia Gibert[1,10], Damiano Porcelli[1,23], Nico Posnien[1,24], Alejandro Sánchez-Gracia[1,20], Sonja Grath[1,25], Élio Sucena[1,26,27], Alan O. Bergland[1,28,§], Maria Pilar Garcia Guerreiro[1,29], Banu Sebnem Onder[1,30], Eliza Argyridou[1,25], Lain Guio[1,5], Mads Fristrup Schou[1,19,22], Bart Deplancke[1,31], Cristina Vieira[1,10], Michael G. Ritchie[1,14], Bas J. Zwaan[1,32], Eran Tauber[1,33], Dorcas J. Orengo[1,20], Eva Puerma[1,20], Montserrat Aguadé[1,20], Paul S. Schmidt[1,34,§], John Parsch[1,25], Andrea J. Betancourt[1,35], Thomas Flatt[1,2,3,†,*,§], Josefa González[1,5,†,*,§]

[1] The European *Drosophila* Population Genomics Consortium (*DrosEU*)

[2] Department of Ecology and Evolution, University of Lausanne, CH-1015 Lausanne, Switzerland

[3] Department of Biology, University of Fribourg, CH-1700 Fribourg, Switzerland

[4] Current affiliations: Department of Evolutionary Biology and Environmental Sciences, University of Zürich, CH-8057 Zürich, Switzerland; Department of Cell and Developmental Biology, Medical University of Vienna, AT-1090 Vienna, Austria

[5] Institute of Evolutionary Biology, CSIC-Universitat Pompeu Fabra, Barcelona, Spain

[6] Department of Evolutionary Biology and Ecology, University of Freiburg, 79104 Freiburg, German

[7] Instituto de Biologia Molecular e Celular (IBMC) University of Porto, Porto, Portugal

[8] Instituto de Investigação e Inovação em Saúde (I3S), University of Porto, Porto, Portugal

[9] Institute of Evolutionary Biology, University of Edinburgh, Edinburgh, United Kingdom

[10] Laboratoire de Biométrie et Biologie Evolutive, UMR CNRS 5558, University Lyon 1, Lyon, France

[11] Department of Molecular Biology and Genetics, 107 Biotechnology Building, Cornell University, Ithaca, New York 14853, USA

[12] Research and Innovation Centre, Fondazione Edmund Mach, San Michele all' Adige, Italy

[13] Department of Biological and Environmental Science, University of Jyväskylä, Jyväskylä, Finland

[14] Centre for Biological Diversity, School of Biology, University of St. Andrews, St Andrews, United Kingdom

[15] Evolutionary Biology, Zoological Institute, University of Basel, Basel, CH-4051, Switzerland

[16] General and Medical Genetics Department, Taras Shevchenko National University of Kyiv, Kyiv, Ukraine

[17] State Institution National Antarctic Center of Ministry of Education and Science of Ukraine, 16 Taras Shevchenko Blvd., 01601, Kyiv, Ukraine

[18] Laboratory of Genome Variation, Institute of Molecular Genetics of RAS, Moscow, Russia

[19] Department of Bioscience - Genetics, Ecology and Evolution, Aarhus University, Aarhus C, Denmark

[20] Departament de Genètica, Microbiologia i Estadística, Facultat de Biologia and Institut de Recerca de la Biodiversitat (IRBio), Universitat de Barcelona, Barcelona, Spain

[21] Laboratoire Evolution, Génomes, Comportement et Ecologie (EGCE) UMR 9191 CNRS - UMR247 IRD - Université Paris Sud - Université Paris Saclay. 91198 Gif sur Yvette Cedex, France.

[22] Department of Biology, Section for Evolutionary Ecology, Lund, Sweden

[23] Department of Animal and Plant Sciences, Sheffield, United Kingdom

[24] Universität Göttingen, Johann-Friedrich-Blumenbach-Institut für Zoologie und Anthropologie, Göttingen, Germany

[25] Division of Evolutionary Biology, Faculty of Biology, Ludwig-Maximilians-Universität München, Planegg, Germany

[26] Instituto Gulbenkian de Ciência, Oeiras, Portugal

[27] Departamento de Biologia Animal, Faculdade de Ciências da Universidade de Lisboa, Lisboa, Portugal

[28] Department of Biology, University of Virginia, Charlottesville, VA, USA

[29] Departament de Genètica i Microbiologia, Universitat Autònoma de Barcelona, Barcelona, Spain

[30] Department of Biology, Faculty of Science, Hacettepe University, Ankara, Turkey

[31] Laboratory of Systems Biology and Genetics, EPFL-SV-IBI-UPDEPLA, CH-1015 Lausanne, Switzerland

[32] Laboratory of Genetics, Department of Plant Sciences, Wageningen University, Wageningen, Netherlands

[33] Department of Evolutionary and Environmental Biology and Institute of Evolution, University of Haifa, Haifa, Israel

[34] Department of Biology, University of Pennsylvania, Philadelphia, USA

[35] Institute of Integrative Biology, University of Liverpool, Liverpool, United Kingdom

[†] **For correspondence**: martin.kapun@uzh.ch, thomas.flatt@unifr.ch, josefa.gonzalez@ibe.upf-csic.es,

[*] These authors contributed equally to this work

[§] Members of the *Drosophila* Real Time Evolution (Dros-RTEC) Consortium

**Competing interests**: The authors declare that no competing interests exist.

## Abstract

Genetic variation is the fuel of evolution but analysing the spatio-temporal dynamics of genetic changes in natural populations is challenging, comprehensive sampling logistically difficult, and sequencing of entire populations costly. Here we address these issues by performing the first continent-wide genomic analysis of genetic variation in European *Drosophila melanogaster*, based on 48 pool-sequencing samples from 32 populations. Our analyses uncover a novel pattern of major longitudinal population structure; establish previously unknown clines in inversions and transposable elements across Europe; and provide evidence for non-local, continent-wide selective sweeps that are shared among the majority of populations. We also find pronounced variation among populations in the composition of the fly microbiome and identify five new DNA viruses adding to a single example known so far for this species. Our study has important implications for the evolution and demography of *D. melanogaster*, an ancestrally African species that first colonized Europe before becoming cosmopolitan.

Keywords: *P*opulation genomics, demography, selection, clines, SNPs, structural variants, symbionts, viruses.

## Introduction

Studying the processes that create and maintain genetic variation in natural populations is fundamental to understanding the process of evolution (Dobzhansky 1970; Lewontin 1974; Kreitman 1983; Kimura 1984; Hudson *et al.* 1987; McDonald & Kreitman 1991; Adrian & Comeron 2013). Until recently, technological constraints have limited studies of natural genetic variation to small genomic regions and small numbers of individuals. With the development of population genomics, we can now analyse patterns of genetic variation on a genome-wide scale for large numbers of individuals, with sampling structured across space and time. As a result, we have gained fundamental new insights into evolutionary dynamics of genetic variation in natural populations (e.g., Hohenlohe *et al.* 2010; Cheng *et al.* 2012; Begun *et al.* 2007; Pool *et al.* 2012; Harpur *et al.* 2014; Zanini *et al.* 2015). Despite this recent technological progress, extensive large-scale sampling and genome sequencing of populations remains prohibitively expensive in terms of cost and labor for any individual research group.

Here, we present the first comprehensive, continent-wide genomic analysis of genetic variation in European *Drosophila melanogaster*, based on 48 pool-sequencing samples from 32 populations collected in 2014 (Figure 1) by the European *Drosophila* Population Genomics Consortium (*DrosEU*; https://droseu.net). *D. melanogaster* offers several advantages for studying the relevant spatio-temporal scales of evolution: a relatively small genome, a broad geographic range, a multivoltine life history that allows sampling across

126 generations over short timescales, ease of sampling natural populations using
127 standardized techniques, and a well-developed context for population genomic analysis
128 (e.g., Powell 1997; Keller 2007; Hales *et al.* 2015). Importantly, this species is studied by
129 an extensive research community, with a long history of developing shared resources
130 (Larracuente & Roberts 2015; Bilder & Irvine 2017).
131
132 The current study complements and extends previous studies of genetic variation in *D.*
133 *melanogaster*, both from its native range in sub-Saharan Africa and from its world-wide
134 expansion as a human commensal into Europe 10–20,000 years ago and into North
135 America and Australia in the last few centuries (e.g., Lachaise *et al.* 1988; David & Capy
136 1988; Li & Stephan 2006; Keller 2007; Sprengelmeyer et al 2018; Arguello *et al.* 2019;
137 also cf. Kapopoulou *et al.* 2018a). The colonization of novel habitats and climate zones on
138 multiple continents makes *D. melanogaster* especially powerful for studying parallel local
139 adaptation. Previous studies of genomic variation have uncovered latitudinal clines in
140 allele frequencies (e.g., Schmidt & Paaby 2008; Turner *et al.* 2008; Kolaczkowski *et al.*
141 2011b; Fabian *et al.* 2012; Bergland *et al.* 2014; Machado *et al.* 2016; Kapun *et al.* 2016a),
142 structural variants such as chromosomal inversions (reviewed in Kapun & Flatt 2019),)
143 transposable elements (TEs) (Boussy *et al.* 1998; González *et al.* 2008; 2010), and
144 complex phenotypes (de Jong & Bochdanovits 2003; Schmidt & Paaby 2008; Schmidt *et*
145 *al.* 2008; Kapun *et al.* 2016b; Behrman *et al.* 2018). Thus far, sampling across these
146 latitudinal gradients has been restricted to single transects on the east coasts of Australia
147 and North America; in addition to parallel local adaptation, clines on these continents may
148 be due to admixture between cohorts of flies with different colonization histories (Caracristi
149 & Schlötterer 2003; Yukilevich & True 2008a; b; Duchen *et al.* 2013; Kao *et al.* 2015;
150 Bergland *et al.* 2016).

In contrast, the population genomics of *D. melanogaster* on the European continent remains largely uncharacterized (Božičević *et al.* 2016; Pool *et al.* 2016; Mateo *et al.* 2018). Because Eurasia was the first continent colonized by *D. melanogaster* as they migrated out of Africa, we sought to understand how this species has adapted to new habitats and climate zones in Europe, where it has been established the longest (Lachaise *et al.* 1988; David & Capy 1988). We analyse our data at three levels: (1) variation at single-nucleotide polymorphisms (SNPs) in nuclear and mitochondrial (mtDNA) genomes (~5.5 x $10^6$ SNPs in total); (2) structural variation, including TE insertions and chromosomal inversions; and (3) variation in the microbiota associated with flies, including bacteria, fungi, protists, and viruses.

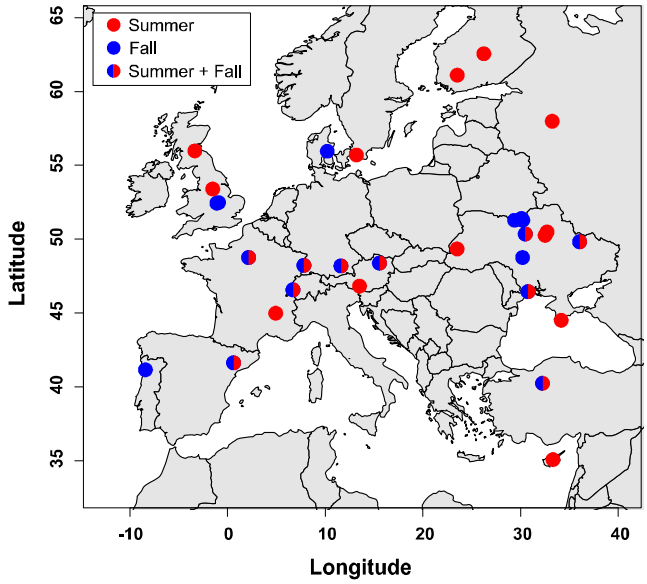


**Figure 1. The geographic distribution of population samples.** Locations of all samples in the 2014 *DrosEU* data set. The color of the circles indicates the sampling season for each location: ten of the 32 locations were sampled at least twice, once in summer and once in fall (see Table 1 and Supplemental Table 1). Note that some of the 12 Ukrainian locations overlap in the map.

## Results

As part of the *DrosEU* consortium, we collected 48 population samples of *D. melanogaster* from 32 geographical locations across Europe in 2014 (Table 1; Figure 1). We performed pooled sequencing (Pool-Seq) of all 48 samples, with an average autosomal coverage ≥50x (Table S1). Of the 32 locations, 10 were sampled at least once in summer and once in fall (Figure 1), allowing a preliminary analysis of seasonal change in allele frequencies on a genome-wide scale.

### European and other derived populations exhibit similar amounts of genetic variation

For each sample, we estimated genome-wide levels of nucleotide diversity ($\pi$ and Watterson's $\theta$, corrected for pooling; Futschik 2010; Kofler *et al.* 2011). We find that most European populations have similar levels of genetic variation (Table S1). Moreover, our estimates of pairwise nucleotide diversity are similar to those from derived non-African (North American and Australian) populations, whether sequenced as individuals or as pools (Figure 2 and Table S2). Thus, although European populations are considerably older than North American and Australian populations, they exhibit similar levels of DNA sequence variability.

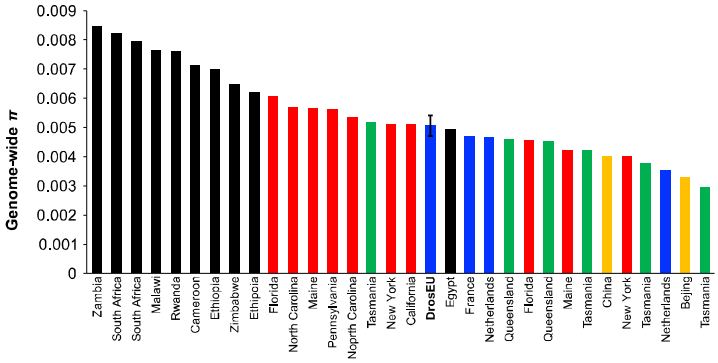


**Figure 2. Genetic variation in worldwide samples.** Bar plot showing the distribution of genome-wide estimates of Tajima's $\pi$ of the *DrosEU* and other genomic datasets (also see Table S2 and Materials and Methods) The error bar in the *DrosEU* dataset represent the standard deviation of $\pi$ across all 48 population samples.

We next tested for associations between geographic variables and genome-wide average levels of genetic variation. We found that neither $\pi$ nor $\theta$ was correlated with latitude or longitude, but both strongly decreased with altitude (Table 2). This contrasts with previous studies of flies collected from a broader range of altitudes, which found increased genetic diversity in high-elevation populations (Lian *et al.* 2018). Finally, we tested for a correlation between genome-wide variation and the season of collection, finding no relationship (Table 2). Together, these results suggest that there is little spatio-temporal variation among European populations in overall levels of sequence variability.

For all populations, the ratio of *X*-linked to autosomal variation ($\pi_X/\pi_A$) was well below the value of 0.75 expected under neutrality with equal sex ratios (ranging from 0.53 to 0.66, one-sample Wilcoxon rank test, $p < 0.001$). These estimates are broadly consistent with those from previous studies of European and other non-African populations (e.g. Andolfatto 2001; Kauer *et al.* 2002; Hutter *et al.* 2007; Betancourt *et al.* 2004; Mackay *et al.* 2012; Langley *et al.* 2012). Surprisingly, the $\pi_X/\pi_A$ ratio increased significantly, significantly, albeit weakly, with latitude (Spearman's  = 0.315, p = 0.0289). This observation is at odds with a the predictions of a simple model of periodic bottlenecks leading to a lower X/A ratio in northern populations (Hutter *et al.* 2007; Pool & Nielsen 2007), but might be consistent with stronger selection or more male-biased sex-ratios in the south as compared to the north (Charlesworth 2001; Hutter *et al*. 2007).

Genetic variation was heterogeneous across the genome, as has been previously reported (Begun & Aquadro 1992; Mackay *et al.* 2012; Langley *et al.* 2012; Huang *et al.* 2014). Both $\pi$ and $\theta$ were markedly reduced close to centromeric and telomeric regions (Figure 3), and strongly positively correlated with recombination rate (linear regression against fine-scale

recombination rate estimates from Comeron *et al.* (2012), $p < 0.001$; not accounting for autocorrelation; Table S3). Recombination rate explained 41–47% and 31–38% of the variation in $\pi$, for the autosomes and X chromosome, respectively. Using broad-scale recombination rate estimates (Fiston-Lavier *et al.* 2010) yielded a qualitatively similar, but slightly stronger correlation in autosomes and weaker in the X chromosome (Figure 3, Table S3, Figure 3 - figure supplement 1).

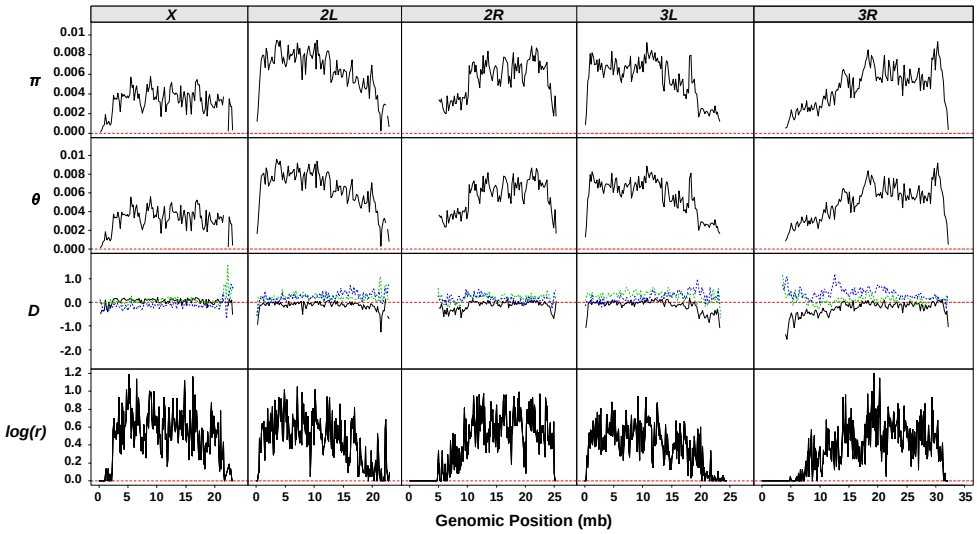


**Figure 3** with 1 supplement**. Genome-wide estimates of genetic diversity and recombination rates**. The distribution of Tajima's $\pi$, Watterson's $\theta$ and Tajima's $D$ (from top to bottom) in 200 kb non-overlapping windows plotted for each chromosomal arm separately. The dashed blue and green lines show estimates for 14 individuals from Rwanda and Zambia, respectively. Bold black lines depict statistics, that were averaged across all 48 samples and the upper and lower grey areas show the corresponding standard deviations for each window. Red dashed lines highlight the vertical position of a zero value. The bottom row shows log-transformed recombination rates ($r$) in 100 kb non-overlapping windows as obtained from Comeron et al. (2010).

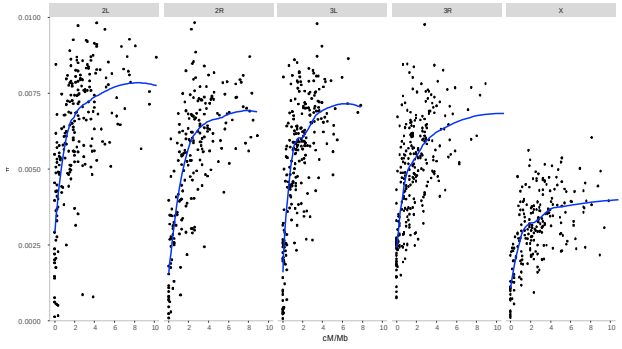


**Figure 3 - figure supplement 1. Correlation between recombination and genetic diversity.** Smooth local regression (LOESS) between recombination rate in cM/Mb (Comeron et al. 2012) and the average of the 48 samples' genetic diversity ($\pi$) in 100 kb non-overlapping windows by chromosome arm.

In contrast to $\pi$ and $\theta$, the European populations showed major differences in mean Tajima's *D* (Table S1). Tajima's *D* measures deviations from neutral expectations in allele frequencies, which can be due either to selection or complex demography, with negative *D* indicating an excess of low-frequency variants (Tajima 1983). Approximately half of the European samples have negative *D*, It is possible that this result is artefactual, caused by heterogeneity in the proportion of sequencing errors among multiplexed sequencing runs. However, this is unlikely, because including sequence run as a covariate in the statistical model did not improve its fit (Supplementary File 2; Table S4). In all of these analyses, we controlled for confounding effects of spatio-temporal autocorrelations between samples by accounting for similarity among spatial neighbors (Moran's $I \approx 0$, $p > 0.05$ for all tests). When comparing *D* in European samples with ancestral African populations from Zambia and Rwanda, the values were generally lower in the European populations, possibly due to the recent range and population size expansion (Figure 3 and Table S5). Similar to genetic diversity, *D* was also heterogeneous across the genome. Tajima's *D* was broadly reduced in the vicinity of telomeric and centromeric regions, possibly reflecting extended purifying selection or selective sweeps close to heterochromatic regions, and due to reduced recombination.

**Several genomic regions show signatures of continent-wide selective sweeps**

Genomic regions that show localized reductions in Tajima's *D* are attractive candidates for having undergone recent selective sweeps. To identify such genomic regions, we used *Pool-hmm* (Boitard *et al.* 2013; Table S6A), which – like Tajima's *D* – identifies candidate sweep regions *via* distortions in the allele frequency spectrum. Several genomic regions identified in this way coincide with previously identified, well-supported sweeps in the proximity of *Hen1* (Kolaczkowski *et al.* 2011b), *Cyp6g1* (Daborn *et al.* 2002), *wapl*

(Beisswanger *et al.* 2006), and around the chimeric gene *CR18217* (Rogers & Hartl 2012), among others (Table S6B). These regions also showed local reductions in Tajima's *D* and genetic variation, again consistent with selection (Figure 4 and Figure 4-figure supplement 1 and 2). The putative sweep regions included 145 of the 232 genes previously identified using *Pool-hmm* in an Austrian population (Boitard et al 2012; Table S6C). Other regions identified have not previously been described as harboring sweeps; these represent potential novel targets of positive selection deserving of further investigation (Table S6A). Overall, we identified 64 genes that showed signatures of selection across all European populations analysed (Table S6D); thirty-five of them were located in regions with low Tajima's *D*. This pattern suggests the existence of continent-wide sweeps that either predate the colonization of Europe (e.g., Beisswanger *et al.* 2006), or that have swept across the majority of European populations more recently (Table S6D). Finally, we classified the populations according to the Köppen-Geiger climate classification (Peel *et al.* 2007) and identified several candidate sweeps exclusive to arid, temperate or cold regions; Table S6A). For temperate climates, candidate sweep regions were enriched for functions such as 'response to stimulus', 'transport', and 'nervous system development'; for cold climates, they were enriched for 'vitamin and co-factor metabolic processes' (Table S6E). In contrast, we did not find any significant GO enrichment for arid candidate sweep regions. In summary, this dataset represents a rich genomic resource for future in-depth studies of selective sweeps and adaptation to different climates in *Drosophila*.

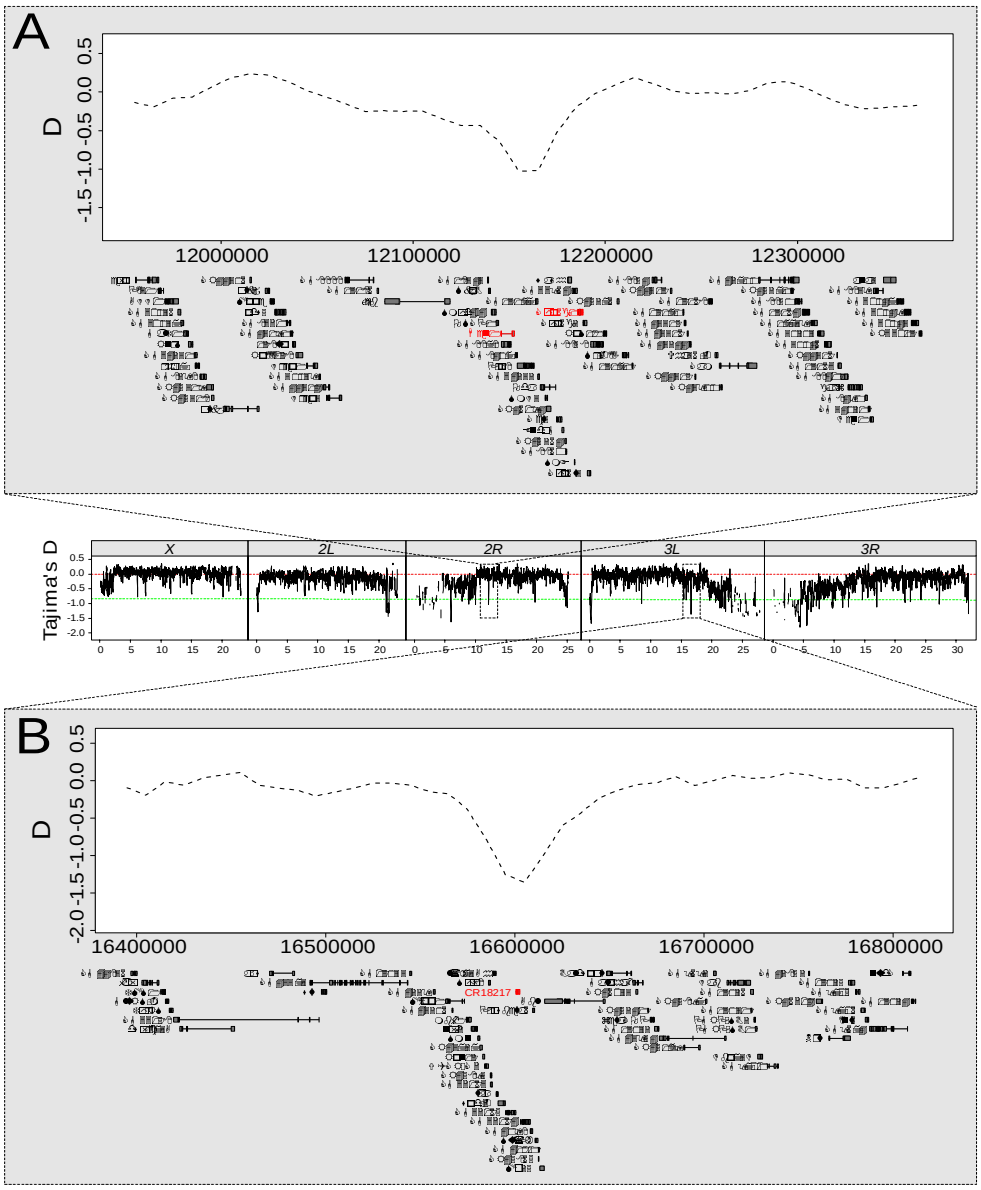


**Figure 4** with 2 supplements. **Signals of selective sweeps.** The central panel shows the distribution of Tajima's *D* in 50 kb sliding windows with 40 kb overlap, with red and green dashed lines indicating Tajima's *D* = 0 and -1, respectively. The top panel shows a detail of a genomic region on chromosomal arm *2R* in the vicinity of *Cyp6g1* and *Hen1* (highlighted in red), genes reportedly involved in pesticide resistance. This strong sweep signal is characterized by an excess of low-frequency SNP variants and overall negative Tajima's *D* in all samples. Coloured solid lines depict Tajima's *D* for each sample (see SI Figure 4 for color codes); the black dashed line shows Tajima's *D* averaged across all samples. The bottom panel shows a region on *3L* previously identified as a potential target of selection, which shows a similar strong sweep signature. Notably, both regions show strongly reduced genetic variation (Figure 4 - figure supplement 1).

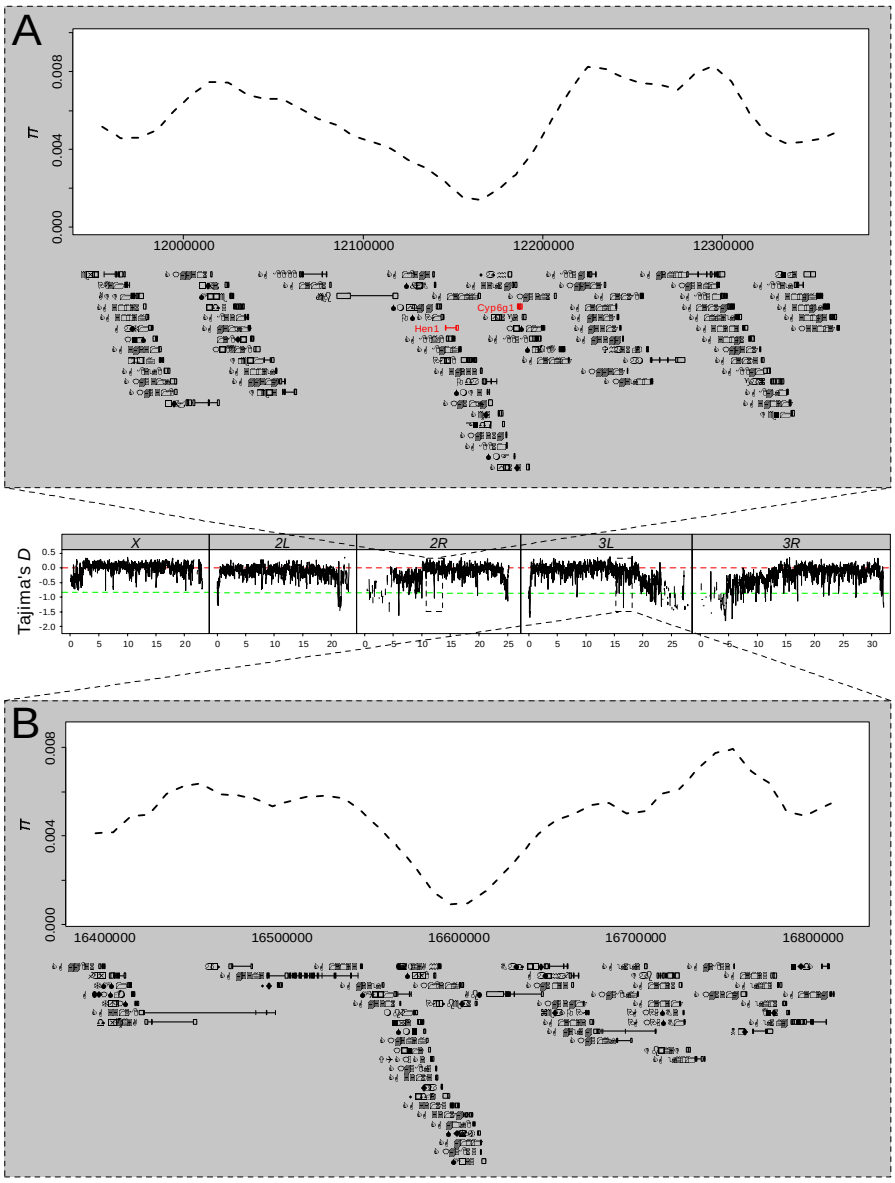


**Figure 4 - figure supplement 1: Genetic variation in regions of putative selective sweeps.** This figure is equivalent to Figure 4 in the main text but shows the distribution of genetic variation *(π)* in regions with depressed Tajima's *D* around the well-studied *Cyp6g1* locus (A) and around a previously known candidate region on *3L* (B). Similar to Tajima's *D*, *π* was calculated in 50 kb sliding windows with 40 kb overlap. See Table S6 for more examples. A legend for the color codes of the samples can be found in Figure 4 - figure supplement 2.

| | | |
|---|---|---|
| AT_14_Mau_1 | UA_14_Ode_19 | ES_14_Lle_35 |
| AT_14_Mau_2 | UA_14_Ode_20 | FI_14_Aka_36 |
| TR_14_Yes_3 | UA_14_Ode_21 | FI_14_Aka_37 |
| TR_14_Yes_4 | UA_14_Ode_22 | FI_14_Ves_38 |
| FR_14_Vil_5 | UA_14_Kyi_23 | DK_14_Kar_39 |
| FR_14_Vil_7 | UA_14_Kyi_24 | DK_14_Kar_41 |
| FR_14_Got_8 | UA_14_Var_25 | CH_14_Cha_42 |
| UK_14_She_9 | UA_14_Pyr_26 | CH_14_Cha_43 |
| UK_14_Sou_10 | UA_14_Dro_27 | AT_14_See_44 |
| CY_14_Nic_11 | UA_14_Cho_28 | UA_14_Kha_45 |
| UK_14_Mar_12 | UA_14_Cho_29 | UA_14_Kha_46 |
| UK_14_Lut_13 | SE_14_Lun_30 | UA_14_Cho_47 |
| DE_14_Bro_14 | DE_14_Mun_31 | UA_14_Cho_48 |
| DE_14_Bro_15 | DE_14_Mun_32 | UA_14_Kyi_49 |
| UA_14_Yal_16 | PT_14_Rec_33 | UA_14_Uma_50 |
| UA_14_Yal_18 | ES_14_Lle_34 | RU_14_Vald_51 |

**Figure 4 - figure supplement 2.** Legend for color code in Figure 4, Figure 4 - figure supplement 1.

## European populations are structured along an east-west gradient

We next investigated patterns of genetic differentiation due to demographic substructure. Overall, pairwise differentiation as measured by $F_{ST}$ was relatively low, particularly for the autosomes (autosomal $F_{ST}$ 0.013–0.059; *X*-chromosome $F_{ST}$: 0.043–0.076; Mann-Whitney-U test; $p < 0.001$; Table S1). The slightly elevated $F_{ST}$ for the *X* chromosome is expected given its smaller effective population size (Hutter *et al.* 2007). One population, from Sheffield (UK), was unusually differentiated from the others (Table S1) and was excluded from analyses of neutral genetic differentiation. Despite overall low levels of among-population differentiation, European populations showed evidence of geographic substructure. To analyse this pattern in detail, we focused on SNPs most likely to reflect neutral population structure, those at 4-fold degenerate sites, in regions outside those showing signatures of selective sweeps, in regions of high recombination ($r$ > 3cM/Mb; Comeron et al. 2011) and at least 1 Mb away from the breakpoints of common inversions.

313 The final filtered data set consisted of 8,727 SNPs. Within Europe, we found a weak but
314 significant pattern of isolation by distance (IBD). That is, pairwise $F_{ST}$, though low overall,
315 increased significantly with geographic distance (Mantel test; $p < 0.001$; $r$=0.65, max. $F_{ST}$ ~
316 0.05; Figure 5A and Figure 5A – figure supplement 1A).
317

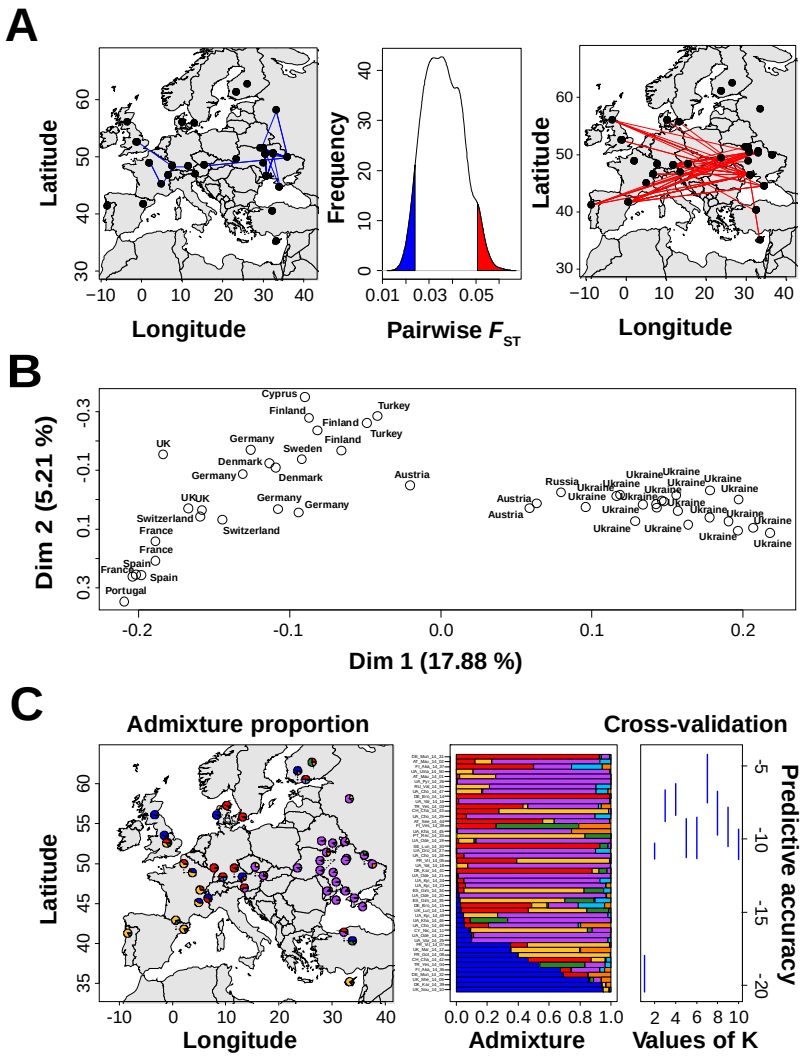


318

319 **Figure 5** with 1 supplement**. Genetic differentiation among European populations**. (A) Average $F_{ST}$ among
320 populations at putatively neutral sites. The centre plot shows the distribution of $F_{ST}$ values for all 1,128 pairwise
321 population comparisons, with the $F_{ST}$ values for each comparison obtained from the mean across all 8,727 SNPs used in
322 the analysis. Plots on the left and the right show population pairs in the lower (blue) and upper (red) 5% tails of the $F_{ST}$
323 distribution. (B) PCA analysis of allele frequencies at the same SNPs reveals population substructuring in Europe.
324 Hierarchical model fitting using the first four PCs showed that the populations fell into three clusters (indicated by colour),
325 with cluster assignment of each population subsequently estimated by *k*-means clustering. (C) Admixture proportions for
326 each population inferred by model-based clustering with *ConStruct* are highlighted as pie charts (left plot) or Structure
327 plots (centre). The optimal number of 7 spatial layers (K) was inferred by cross-validation (right plot).

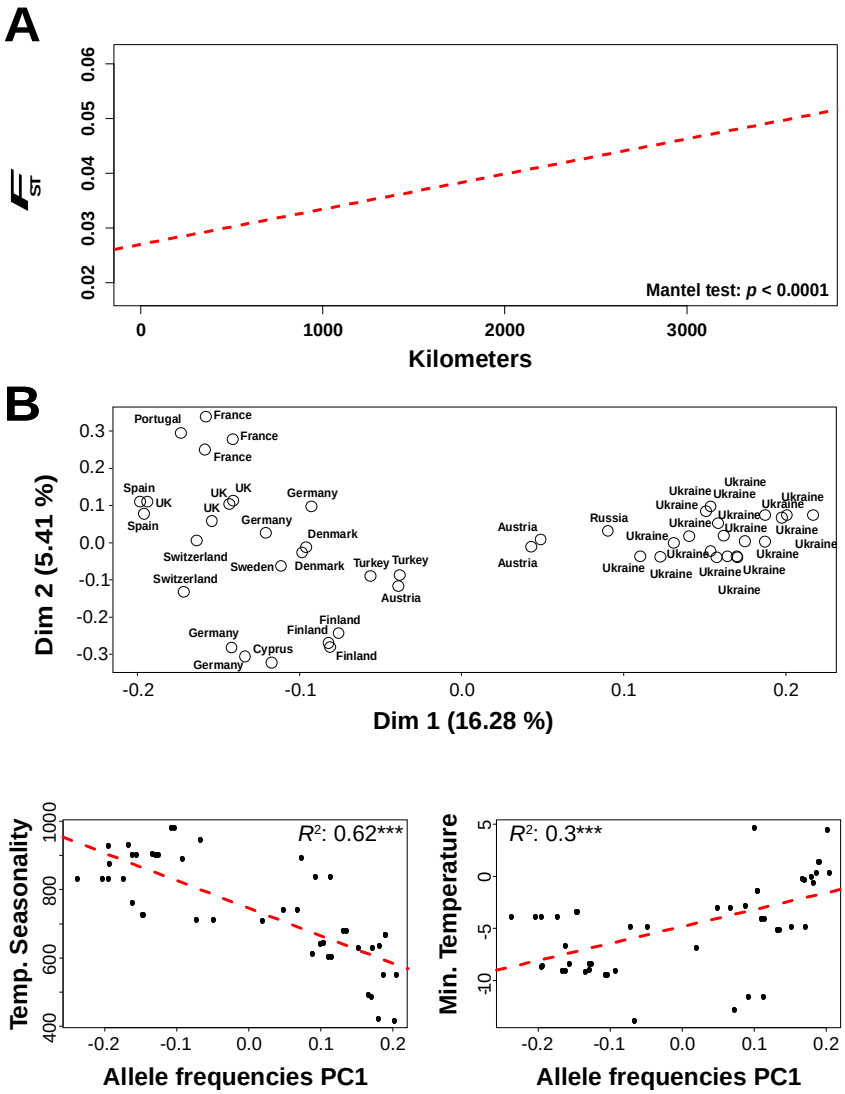


**Figure 5 - figure supplement 1:** Genetic differentiation among European populations. (A) Average $F_{ST}$ for 8,727 putatively neutral SNPs is significantly negatively correlated with geographic distance (red dashed line shows the linear regression) (B) PCA-based inference of population structure similar to Figure 5B in the main text, but based on 20,008 SNPs located in short introns (<60bp). (C) We tested the top 5 PC for significant associations with 8 climatic variables obtained from the WorldClim database; the two significant regressions, between PC1 and Temperature seasonality (WorldClim Biovar 4; left) and between PC1 and minimum temperature of the coldest month (WorldClim Biovar 6; right) are shown.

We investigated population substructure using principal components analysis (PCA) on allele frequencies from the same set of SNPs at 4-fold degenerate sites. The first three PC axes explained >25% of the total variance (PC1: 17.88%, PC2: 5.2%, PC3: 4.7%, eigenvalues = 410, 101, and 92, respectively), with PC1 strongly correlated with longitude

and to a lesser extent with altitude (Table 2). This longitudinal stratification is expected under a simple model of IBD, as the continent extends further in longitude than latitude. As there was significant spatial autocorrelation between samples (as indicated by Moran's test on residuals from linear regressions with PC1), we repeated the analysis with an explicit spatial error model; the association between PC1 and longitude remained significant. Like PC1, PC2 is correlated with longitude and altitude. PC3, by contrast, is not associated with any variable examined (Table 2). No major PC axes were correlated with season, indicating that there were no shared seasonal differences across samples in our data. However, based on linear regressions comparing summer and fall values of PC1 (adjusted $R^2$: 0.98; $p$-value < 0.001), PC2 ($R^2$: 0.79; $p$-value < 0.001) and PC3 ($R^2$: 0.93; $p$-value < 0.001), we found very strong associations of genetic variation across seasons in the 10 locations that were sampled in summer and fall. This indicates a high degree of spatio-temporal stability in the levels of genetic variation.

Hierarchical model fitting based on the first three PC axes resulted in three distinct clusters (Figure 5B) separated along PC1, supporting the notion of strong longitudinal differentiation among European populations. Importantly, these results remain qualitatively unchanged when restricting the analysis to SNPs located in short introns (< 60 bp), which are also assumed to be relatively unaffected by selection (Figure 5 – figure supplement 1B; Haddrill *et al.* 2005; Singh *et al.* 2009; Parsch *et al.* 2010; Clemente & Vogl 2012; Lawrie *et al.* 2013).

Model-based spatial clustering showed qualitatively similar results, with populations separated mainly by longitude (Figure 5C; using ConStruct, with K=7 spatial layers chosen based on model selection procedure *via* cross-validation). We could also infer levels of

admixture among populations from this analysis; population samples from eastern and northwestern Europe showed low levels of admixture, while those from central Europe appeared locally well-mixed (Figure 5C).

In addition to restricted gene flow between geographic areas, local adaptation may explain population substructuring, even at neutral sites, if closely related populations tend to respond to similar selective pressures. We thus probed whether this spatial substructuring is associated with any of nineteen climatic variables, obtained from the WorldClim database (Hijmans *et al.* 2005). These climatic variables represent averages interpolated averages across more than 50 years of observation at the geographic coordinates corresponding to our sampling locations. Only two variables are significant after Bonferroni correction (adjusted $\alpha = 0.0026$): between PC1 and 'temperature seasonality' (BioVar 4; Hijmans et al. 2005; $R^2 = 0.62$, $P<0.001$; Figure 5 – figure supplement 1C) and between PC1 and 'minimum temperature of the coldest month' ($R^2 = 0.3$, $P<0.001$; Figure 5 – figure supplement 1C). This suggests that the pronounced longitudinal differentiation along the European continent could at least partly be driven by the transition from oceanic to continental climate, leading to gradual changes in temperature seasonality and the severity of winter conditions which might impact demography, especially local survival. To the best of our knowledge, such strongly pronounced longitudinal structure and differentiation on a continent-wide scale has not yet been reported for *D. melanogaster.*

**Mitochondrial haplotypes also exhibit longitudinal population structure**

Our finding that European populations show strong longitudinal structure is also supported by an analysis of mitochondrial haplotypes. We identified two main mitochondrial haplotypes in Europe, separated by 41 mutations (G1.2 and G2.1; Figure 6A), with highly

391 variable frequencies among populations (Figure 6B). Qualitatively, three types of
392 European populations can be distinguished based on these haplotypes: (1) central
393 European populations with a high frequency (> 60%) of the G1 haplotypes, (2) Eastern
394 European populations in summer, with a low frequency (< 40%) of G1 haplotypes, and (3)
395 Iberian and Eastern European populations in fall, with a combined frequency of G1
396 haplotypes between 40-60% (Figure 6 - figure supplement 1A). These results are
397 consistent with analyses of mitochondrial haplotypes from a North American population
398 (Cooper *et al.* 2015) as well as from worldwide samples (Wolff *et al.* 2016), which revealed
399 a high level of haplotype diversity.

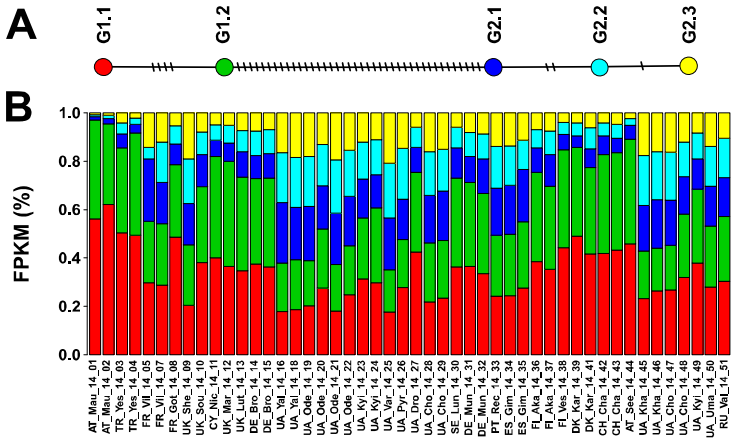


400

401 **Figure 6** with 1 supplement**. Mitochondrial haplotypes.** (A) TCS network showing the relationship of 5 common
402 mitochondrial haplotypes; (B) estimated frequency of each mitochondrial haplotype in 48 European samples.

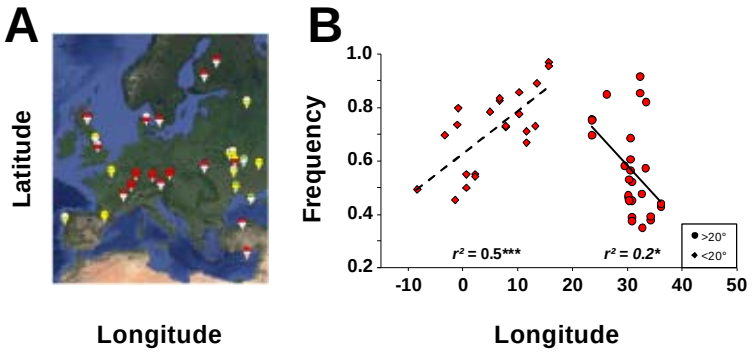


403

404 **Figure 6 - figure supplement 1. Mitochondrial haplotypes.** (A) Graphical summary of the combined frequency of G1

haplotypes in Europe. Summer and Fall are represented at the top and bottom of the circles, respectively. White – no information; green, yellow and red represent a combined frequency of G1 haplotypes lower than 40%, in between 40% and 60% and higher than 60%, respectively. (B) Correlations between the combined frequency of G1 haplotypes and longitude (red diamonds for western populations below 20° and red circles for eastern populations above 20°).

Mitochondrial haplotypes also showed shifts in the relative frequencies of the two haplotype classes between summer and fall, but only in 2 of 9 possible comparisons. While there was no correlation between latitude and the frequency of G1 haplotypes, we found a weak but significant negative correlation between G1 haplotypes and longitude ($r^2$ = 0.10; $p < 0.05$), consistent with the longitudinal east-west population structure observed for SNPs at 4-fold degenerate sites. In a subsequent analysis, we divided the dataset at 20º longitude into an eastern and a western subset because in northern Europe 20º longitude corresponds to the division of two major climatic zones, temperate and cold (Peel *et al.* 2007). This split revealed a clear correlation between longitude and the combined frequency of G1 haplotypes, explaining as much as 50% of the variation in the western group (Figure 6 - figure supplement 1B). Similarly, in eastern populations, longitude and the combined frequency of G1 haplotypes were correlated, explaining approximately 20% of the variance (Figure 6 - figure supplement 1B). Thus, these data on mitochondrial haplotypes clearly confirm the pronounced east-west structure and differentiation among European populations of *D. melanogaster*.

**The frequency of polymorphic TEs varies with longitude and altitude**

To examine the population genetics of structural variants, we first focused on transposable elements (TEs). The repetitive content of the 48 samples ranged from 16% to 21% with respect to nuclear genome size (Figure 7). The vast majority of detected repeats were TEs, mostly represented by long terminal repeats (LTR) and long interspersed nuclear elements (LINE), as well as a few DNA elements (Class II). LTRs best explained total TE

content (LINE+LTR+DNA) (Pearson's $r = 0.87$, $p < 0.01$, *vs.* DNA $r = 0.58$, $p = 0.0117$, and LINE $r = 0.36$, $p < 0.01$ and Figure 7- figure supplement 1A).

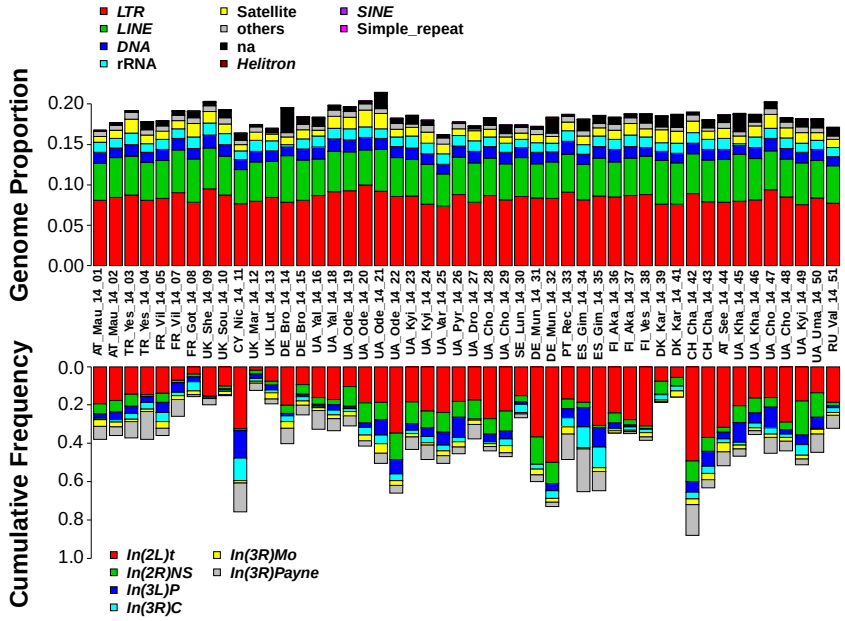


**Figure 7** with 2 supplements. **Geographic patterns in structural variants**. The upper panel shows stacked bar plots with the relative abundances of TEs in all 48 population samples**.** The proportion of each repeat class was estimated from sampled reads with dnaPipeTE (2 samples per run, 0.1X coverage per sample). The lower panel shows stacked bar plots depicting absolute frequencies of six cosmopolitan inversions in all 48 population samples.

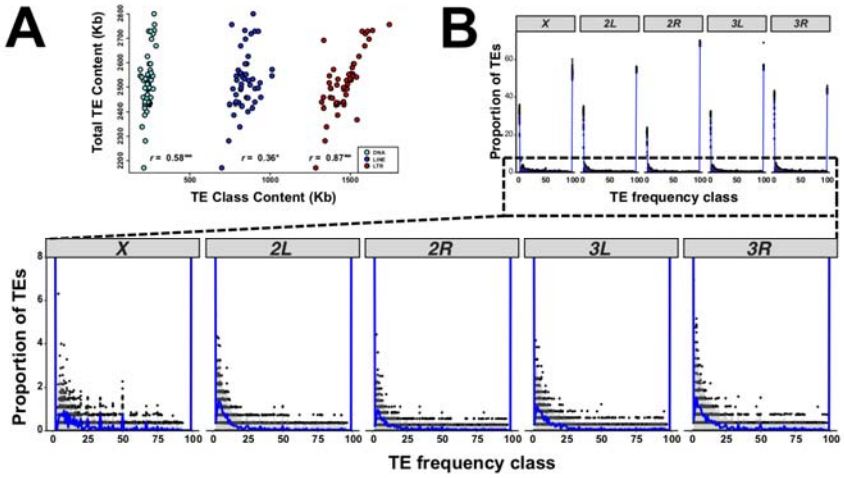


**Figure 7- figure supplement 1**. **Transposable Elements genome content and frequency distributions.** (A) Pearson's correlations between each main TE class (LTR, LINE and DNA) and the total TE content of each pool (LTR+LINE+DNA) in kb. (B) The site frequency spectrum of TE frequencies per chromosome arm. Each dot represents the proportion of TEs in each bin per sample and a smoother geometric line had been added to highlight the trend. Lower panel is a zoom in of the above panel.

We next estimated population frequencies of 1,630 TE insertions annotated in the *D. melanogaster* reference genome *v.6.04* using *T-lex2* (Table S7, Fiston-Lavier *et al.* 2015). On average, 56% of the TEs annotated in the reference genome were fixed in all samples. The majority of the remaining polymorphic TEs segregated at low frequency in all samples (Figure 7 - figure supplement 1A), potentially due to the effect of purifying selection (González *et al.* 2008; Petrov *et al.* 2011; Kofler *et al.* 2012; Cridland *et al.* 2013; Blumenstiel *et al.* 2014). However, we also observed 142 TE insertions present at intermediate (>10% and <95%) frequencies, which might be consistent with transposition-selection balance (Figure 7 - figure supplement 1B; Charlesworth *et al.* 1994).

In each of the 48 samples, TE frequency and recombination rate were negatively correlated on a genome-wide level (Spearman rank sum test; $p < 0.01$), as previously reported (Bartolomé *et al.* 2002; Petrov *et al.* 2011; Kofler *et al.* 2012). This pattern still held when only polymorphic TEs (population frequency <95%) were analysed, although it was not statistically significant for some chromosomes and populations (Table S8). In either case, the correlation was more negative when using broad-scale (Fiston-Lavier *et al.* 2010), rather than fine-scale (Comeron et al 2012), recombination rate estimates, indicating that broad-scale recombination patterns may best capture long-term population recombination patterns (Materials and methods, Tables S8).

We further tested whether the distribution of TE frequencies among samples could be explained by geographical or temporal variables. We focused on the 141 TE insertions that showed frequency variability among samples (interquartile range, (IQR) > 10; see Materials and Methods) and were located in regions of non-zero recombination according to both fine-scale (Comeron et al. 2012), and broad-scale (Fiston-Lavier et al. (2010)

estimations. Of these, 57 TEs showed significant associations with geographical or temporal variables after multiple testing correction (Table S9). We found significant correlations of 13 TEs with longitude, 13 with altitude, five with latitude, and three with season (Table S9). In addition, the frequencies of the other 23 insertions were significantly correlated with more than one of the above-mentioned variables. These TEs were scattered along the five main chromosome arms, with the majority located inside genes (42 out of 57; Table S9).

Two TE families were enriched in the 57 TE dataset: the LTR *297* family with 11 copies, and the DNA *pogo* family with five copies ($\chi^2$-values after Yate's correction < 0.05; Table S10). Interestingly, 14 of these 57 TEs coincide with previously identified adaptive candidate TEs, suggesting that our dataset might be enriched for adaptive insertions, several of which seem to exhibit spatial frequency clines (Table S9; Rech *et al*. 2019).

**Inversions exhibit latitudinal and longitudinal clines in Europe**

Another class of structural variants, chromosomal inversions, show spatial patterns in North American and Australian populations, potentially due to selection (reviewed in Kapun & Flatt 2019). In contrast to North America and Australia, inversion clines in Europe are poorly characterized (Lemeunier & Aulard 1992). Here, we examined the presence and frequency of six cosmopolitan inversions (*In(2L)t, In(2R)NS, In(3L)P, In(3R)C, In(3R)Mo, In(3R)Payne*) in our European samples, using a panel of inversion-specific marker SNPs (Kapun *et al.* 2014). All samples were polymorphic for one or more inversions (Figure 7). However, only *In(2L)t* segregated at substantial frequencies in most populations (average frequency = 20.2%); all other inversions were either absent or rare (average frequencies: *In(2R)NS* = 6.2%, *In(3L)P* = 4%, *In(3R)C* = 3.1%, *In(3R)Mo* =2.2%,

495 *In(3R)Payne* = 5.7%).

496

497 Despite their overall low frequencies, several inversions exhibited pronounced clinality
498 (Table 3). In particular, we observed significant latitudinal clines for *In(3L)P, In(3R)C* and
499 *In(3R)Payne*. Although they differed in overall frequencies, *In(3L)P* and *In(3R)Payne*
500 showed latitudinal clines in Europe qualitatively similar to clines previously observed along
501 the North American and Australian east coasts (Figure 7 - figure supplement 2 and Table
502 S11, Kapun *et al.* 2016a), which, at least in the case of *In(3R)Payne*, are maintained by
503 spatially varying selection (Kapun *et al*. 2016a,b; Durmaz *et al.* 2018; Anderson *et al.*
504 2005; Umina *et al.* 2005; Kennington *et al.* 2006; Rako *et al.* 2006).

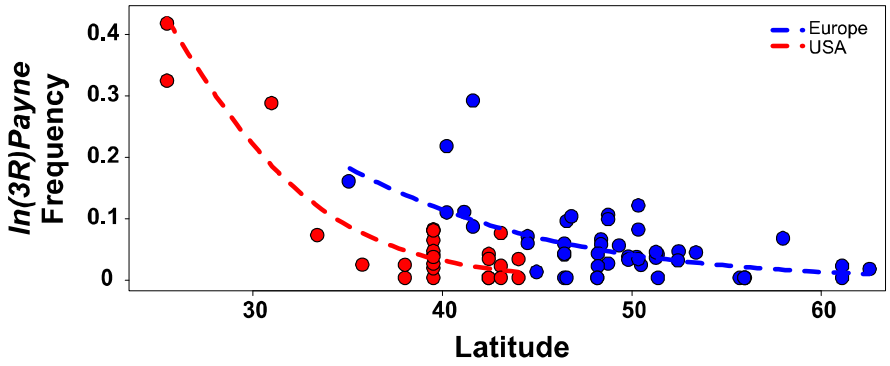


505

506 **Figure 7 - figure supplement 2. Clinal variation of the inversion *In(3R)Payne* across continents.** Parallel frequency
507 clines of *In(3R)Payne* along the latitudinal axis at the North American east coast (red) and in Europe (blue) (see also
508 Table S11).

509

510 We also detected – for the first time – longitudinal clines for *In(2L)t* and *In(2R)NS*, with
511 both polymorphisms decreasing in frequency from east to west, a result consistent with the
512 strong longitudinal population differentiation in Europe. *In(2L)t* also increased in frequency
513 with altitude (Table 3). Except for *In(3R)C,* we did not find significant residual spatio-
514 temporal autocorrelation among samples for any inversion tested (Moran's $I \approx 0$, $p > 0.05$

for all tests; Table 3), suggesting that our analysis was not confounded by spatial autocorrelation for most of the inversions. Further studies are necessary to determine the extent to which these clines of inversion frequencies in Europe are shaped by selection.

**European *Drosophila* microbiomes contain Entomophthora, trypanosomatids and unknown DNA viruses**

We examined the bacterial, fungal, protist, and viral microbiota associated with *D. melanogaster* using the Pool-Seq data. The microbiota can affect life history traits, immunity, hormonal physiology, and metabolic homeostasis of their fly hosts (e.g., Trinder *et al.* 2017; Martino *et al.* 2017).

We characterised the taxonomic origin of the non-*Drosophila* reads in our dataset using MGRAST, which identifies and counts short protein motifs ('features') within reads (Meyer *et al.* 2008). We examined 262 million reads in total and of these most were assigned to *Wolbachia* (mean 53.7%; Figure 8), a well-known endosymbiont of *Drosophila* (Werren *et al.* 2008). The abundance of *Wolbachia* protein features relative to other microbial protein features (relative abundance) varied strongly between samples, ranging from 8.8% in a sample from the UK to almost 100% in samples from Spain, Portugal, Turkey and Russia (Table S12). Similarly, *Wolbachia* loads varied 100-fold between samples, as estimated from the ratio of *Wolbachia* protein features to *Drosophila* protein features (Table S12).

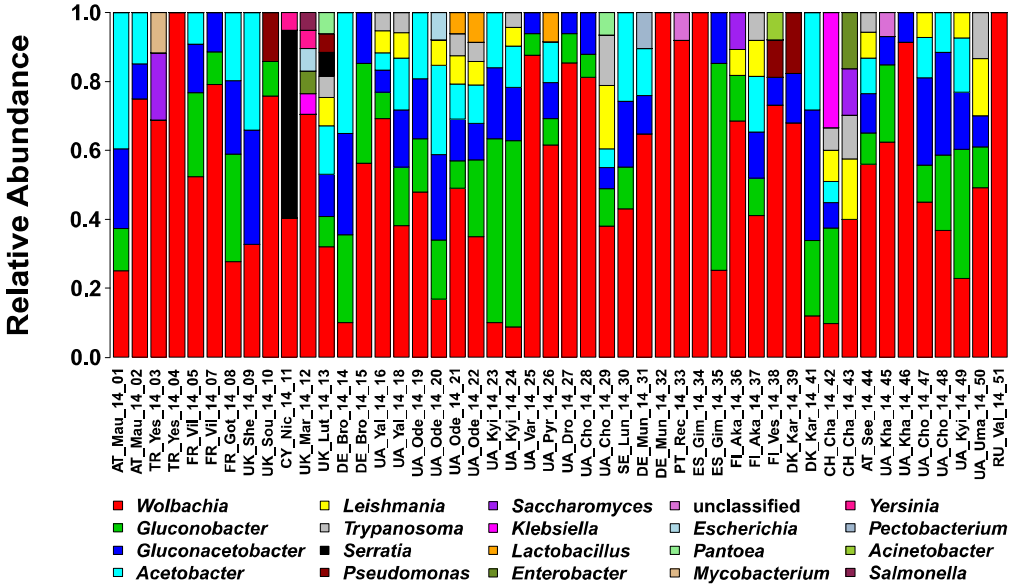


**Figure 8: Microbiome.** Relative abundance of *Drosophila*-associated microbes as assessed by MGRAST classified shotgun sequences. Microbes had to reach at least 3% relative abundance in one of the samples to be represented

Acetic acid bacteria of the genera *Gluconobacter*, *Gluconacetobacter*, and *Acetobacter* were the second largest group, with an average relative abundance of 34.4% among microbial protein features. Furthermore, we found evidence for the presence of several genera of Enterobacteria (*Serratia, Yersinia, Klebsiella, Pantoea, Escherichia, Enterobacter, Salmonella*, and *Pectobacterium*). *Serratia* occurs only at low frequencies or is absent from most of our samples, but reaches a very high relative abundance among microbial protein features in the Nicosia (Cyprus) summer collection (54.5%). This high relative abundance was accompanied by an 80x increase in *Serratia* bacterial load.

We also detected several eukaryotic microorganisms, although they were less abundant than the bacteria. The fraction of fungal protein features, for example, is larger than 3% in only three samples (from Finland, Austria and Turkey; Table S12). Among the eukaryotic microbiota, we found trypanosomatids in 16 samples. Trypanosomatids have been

551 previously reported to be associated with *Drosophila* (Wilfert *et al.* 2011; Chandler &
552 James 2013; Hamilton *et al.* 2015), and this appeared to have been confirmed in this first
553 systematic survey across a wide geographic range in *D. melanogaster*. We also found the
554 fungal pathogen *Entomophthora muscae* in 14 samples (Elya C et al. 2018).
555 Somewhat surprisingly, we found few yeast sequences. Yeasts are commonly found on
556 rotting fruit, the main food substrate of *D. melanogaster*, and have been found in
557 association with *Drosophila* before (Barata *et al.* 2012; Chandler *et al.* 2012). This result
558 suggests that, although yeasts can attract flies and play a role in food choice (Becher *et al.*
559 2012; Buser *et al.* 2014), they might not be highly prevalent in or on *D. melanogaster*
560 bodies but are rather actively digested and thus not part of the microbiome.
561
562 Our data also allowed us to identify DNA viruses. Only one DNA virus has been previously
563 described for *D. melanogaster* (Kallithea virus; Webster *et al.* 2015; Palmer *et al.* 2018)
564 and only two others more from other Drosophilid species (*Drosophila innubila* Nudivirus
565 [Unckless 2011], Invertebrate Iridovirus 31 in *D. obscura* and *D. immigrans* [Webster *et al.*
566 2016]).
567 Here, we found six different DNA viruses, five of which are new (Table S13).
568 Approximately two million reads came from *Kallithea* nudivirus (Webster *et al.* 2015),
569 allowing us to assemble the first complete *Kallithea* genome (>300-fold coverage in the
570 Ukrainian sample UA_Kha_14_46; Genbank accession KX130344). We also identified
571 around 1,000 reads from a novel nudivirus closely related to both *Kallithea* virus and to
572 *Drosophila innubila* nudivirus (Unckless 2011) in sample DK_Kar_14_41 from
573 Karensminde, Denmark (Table S13). As the reads from this virus in our data set were
574 insufficient to assemble the genome, we identified a publicly available dataset
575 (SRR3939042: 27 male *D. melanogaster* from Esparto, California; Machado *et al.* 2016)

576 with sufficient reads to complete the genome (provisionally named "*Esparto* Virus";
577 KY608910).
578 We further identified two novel Densoviruses (*Parvoviridae*). The first is a relative of *Culex*
579 *pipiens* densovirus, provisionally named "*Viltain* virus", found at 94-fold coverage in
580 sample FR_Vil_14_07 (Viltain; KX648535). The second is "*Linvill Road* virus", a relative of
581 *Dendrolimus punctatus* densovirus, represented by only 300 reads here, but with high
582 coverage in dataset SRR2396966 from a North American sample of *D. simulans*
583 (KX648536; Machado *et al.* 2016). In addition, we detected a novel member of the
584 *Bidnaviridae* family,"*Vesanto* virus", a bidensovirus related to *Bombyx mori* densovirus 3
585 with approximately 900-fold coverage in sample FI_Ves_14_38 (Vesanto; KX648533 and
586 KX648534). Finally, in one sample (UA_Yal_14_16) we detected a substantial number of
587 reads from an Entomopox-like virus, which we were unable to fully assemble (Table S13).
588 Using a detection threshold of >0.1% of the *Drosophila* genome copy number, the most
589 commonly detected viruses were *Kallithea* virus (30/48 of the pools) and *Vesanto* virus
590 (25/48), followed by *Linvill Road* virus (7/48) and *Viltain* virus (5/48), with *Esparto* virus
591 being the rarest (2/48).
592

## 593 Discussion

594 In recent years, large-scale population re-sequencing projects have produced major
595 insights into the biology of both model (Mackay *et al.* 2012; Langley *et al.* 2012; Auton et
596 al. 2015; Lack *et al.* 2015; Alonso-Blanco *et al.* 2016; Lack *et al.* 2016) and non-model
597 organisms (e.g., Hohenlohe *et al.* 2010; Wolf *et al.* 2010). In particular, such massive
598 datasets contribute greatly to our growing understanding of the processes that create and
599 maintain genetic variation in natural populations. However, the relevant spatio-temporal

scales for population genomic analyses remain largely unknown (e.g., Guirao-Rico and González 2019). Here we have applied – for the first time – a continent-wide sampling and sequencing strategy to European populations of *D. melanogaster* (Figure 1), allowing us to uncover previously unknown aspects of this species' population biology and evolutionary genetics. This is particularly important because the population genomics of this species in Europe has been poorly characterized to date.

We find that European *D. melanogaster* populations exhibit pronounced longitudinal differentiation. We observed this pattern for a genome-wide set of SNPs at 4-fold degenerate sites, which presumably evolve neutrally (Figure 5), as well as for mitochondrial haplotypes, inversions and TEs which might be subject to spatially varying selection (Figure 6 and 7). Longitudinal differentiation might be due to the transition from oceanic to continental climate along the longitudinal axis (Figure 5-Figure 5 supplement 1). While spatial differences in climatic conditions likely play a major role in driving this pattern, we note that it is remarkably similar to that observed for human populations (e.g., Cavalli-Sforza 1966; Xiao et al. 2004; Francalacci & Sanna 2008; Novembre *et al.* 2008). Indeed, east-west structure has been previously found in sub-Saharan Africa populations of *D. melanogaster*, with the split between eastern and western African populations having occurred ~70 kya ago (Michalakis & Veuille 1996; Aulard *et al.* 2002; Kapopoulou *et al.* 2018b), a period that – interestingly – coincides with a wave of human migration from eastern into western Africa (Nielsen *et al.* 2017). However, in contrast to the pronounced pattern observed in Europe, African east-west structure is relatively weak, explaining only ~2.7% of variation, and is due to an inversion whose frequency varies longitudinally. In contrast, our demographic analyses are based on SNPs located in >1 Mb distance from the breakpoints of the most common inversions. This makes it very unlikely that the strong

longitudinal pattern we have observed is driven by inversions.

Spatial patterns of differentiation were stronger for longitude than for latitude. In contrast, differentiation in North America has mainly been observed across latitude, for both neutral and adaptive polymorphisms (e.g., Machado *et al.* 2016; Kapun *et al.* 2016a; reviewed in Adrion *et al.* 2015). Although our present analysis showed that putatively neutral SNPs were primarily differentiated along longitude, latitudinal clines may still exist for adaptive polymorphisms. In fact, we detected latitudinal frequency clines for both inversions and TEs (Table 3 and Table S9). For the inversions *In(3L)P* and *In(3R)Payne*, the observed latitudinal clines were in qualitative agreement with parallel clines reported from North America and Australia, with the inversions decreasing in frequency as distance from the equator increases (Mettler *et al.* 1977; Knibb *et al.* 1981; Leumeunier & Aulard 1992; Fabian *et al.* 2012; Kapun *et al.* 2014; Rane *et al.* 2015; Kapun *et al.* 2016a). This pattern is widely thought to be a result of climate adaptation, with the inversions containing variants that make them better adapted to tropical or subtropical than to temperate, more seasonal climates (e.g., Kapun *et al*. 2016a). Several euchromatic TE insertions also showed geographic (or seasonal) patterns of variation (Table S9), indicating that they might play a role in local adaptation, particularly since many of them are located in regions where they might affect gene regulation. Further, 17 of them also show significant correlations with either geographical or temporal variables in North American populations (Lerat *et al.* 2019). Additionally, several inversions and TEs also exhibited longitudinal gradients.

We also examined signatures of selective sweeps in our data. Several of the identified regions have previously been reported as potential targets of positive selection (Figure 4,

650 Table S6B and SC). However, most of these sweeps were originally identified by analysing
651 a small number of populations (*e.g.* Kolaczkowski *et al.* 2011b; Daborn *et al.* 2002; Rogers
652 & Hartl 2012). Here, we identified 64 genes (including *wapl*, *CR18217*, and *mgl*) which
653 showed clear signatures of selection and which were widespread across Europe, thus
654 strengthening the case for their adaptive significance. In addition, we found several
655 regions with evidence of hard sweeps, some of them showing evidence of local climatic
656 adaptation (Table S6); these candidate regions represent a valuable resource for future
657 analyses of adaptation in European *Drosophila.*
658
659 Finally, our continent-wide analysis of the microbiota suggests that natural populations of
660 European *D. melanogaster* vary greatly in the composition and abundance of microbes
661 and viruses over space and time. Recent work suggests that at least parts of this variation
662 in microbiomes follows geographic patterns (Walters et al 2018, Wang et al 2019) and
663 contribute to phenotypic differences and local adaptation among populations, especially
664 given that there might be tight and presumably local co-evolutionary interactions between
665 fly hosts and their endosymbionts (e.g., Haselkorn *et al.* 2009; Richardson *et al.* 2012;
666 Staubach *et al.* 2013; Kriesner *et al.* 2016; Wang and Staubach 2018). Most notably, we
667 discovered five new DNA viruses of *D. melanogaster*. Despite this species being host to a
668 wide diversity of RNA viruses, we now have found that the DNA viruses of *D.*
669 *melanogaster* are also widespread, for instance with *Kallithea* virus detected in most
670 populations.
671
672 Our study demonstrates that sampling on a continent-wide scale and pooled sequencing
673 of a large number of natural populations can reveal fundamental and novel aspects of
674 population biology, even for a well-studied model species such as *D. melanogaster*. Our

675 extensive sampling was feasible only due to synergistic collaboration among many
676 research groups. Our efforts in Europe are paralleled in North America by the *Dros-RTEC*
677 consortium, with whom we are collaborating to compare population genomic data across
678 continents. Together, we have sampled both continents annually since 2014; we aim to
679 continue to sample and sequence European and North American *Drosophila* populations
680 with increasing spatio-temporal resolution in future years. With these efforts we hope to
681 provide a rich community resource for biologists interested in molecular population
682 genetics and adaptation genomics.
683

684 ## Materials and methods

685 The 2014 *DrosEU* dataset represents the most comprehensive spatio-temporal sampling
686 of European *D. melanogaster* populations to date (Table 1). It comprises 48 samples of *D.*
687 *melanogaster* collected from 32 geographical locations across Europe at different time
688 points in 2014 through a joint effort of 18 research groups. Collections were mostly
689 performed with baited traps using a standardized protocol (see Supplementary File 2).
690 From each collection, we pooled 33–40 wild-caught males. We used males as they are
691 more easily distinguishable morphologically from similar species than females. Despite our
692 precautions, we identified a low level of *D. simulans* contamination in our sequences; we
693 computationally filtered these sequences from the data prior to further analysis (see
694 below).
695

696 **DNA extraction, library preparation and sequencing**

697 We extracted DNA from each sample after homogenization with bead beating and
698 standard phenol/chloroform extraction. A detailed extraction protocol can be found in the
699 Supplementary File 2. In preparation for sequencing, 500 ng of DNA from each sample

was sheared with a *Covaris* instrument (Duty cycle 10, intensity 5, cycles/burst 200, time 30). Library preparation was performed using *NEBNext Ultra DNA Lib Prep-24* and *NebNext Multiplex Oligos* for Illumina-24 following the manufacturer's instructions. Each sample was sequenced as a pool (Pool-Seq; Schlötterer *et al.* 2014), as paired-end fragments on a *Illumina NextSeq 500* sequencer at the Genomics Core Facility of Pompeu Fabra University. Samples were multiplexed in 5 batches of 10 samples, except for one batch of 8 samples (Table S1). Each multiplexed batch was sequenced on 4 lanes at ~50x raw coverage per sample. The read length was 151 bp, with a median insert size of 348 bp (range 209-454 bp). The data are available from NCBI Bioproject PRJNA388788.

**Mapping pipeline and variant calling**

Prior to mapping, we trimmed and filtered raw FASTQ reads to remove low-quality bases (minimum base PHRED quality = 18; minimum sequence length = 75 bp) and sequencing adaptors using *cutadapt* (v. 1.8.3; Martin 2011). We retained only pairs for which both reads fulfilled our quality criteria after trimming. FastQC analyses of trimmed and quality filtered reads showed overall high base-qualities (median range 29-35), with ~1.36% of bases lost after trimming. We used *bwa mem* (v. 0.7.15; Li 2013) with default parameters to map the trimmed reads. To avoid paralogous mapping, we mapped to a compound reference, consisting of the genomes of *D. melanogaster* (v.6.12) and common commensals and pathogens, including *Saccharomyces cerevisiae* (GCF_000146045.2), *Wolbachia pipientis* (NC_002978.6), *Pseudomonas entomophila* (NC_008027.1), *Commensalibacter intestine* (NZ_AGFR00000000.1), *Acetobacter pomorum* (NZ_AEUP00000000.1), *Gluconobacter morbifer* (NZ_AGQV00000000.1), *Providencia burhodogranariea* (NZ_AKKL00000000.1), *Providencia alcalifaciens* (NZ_AKKM01000049.1), *Providencia rettgeri* (NZ_AJSB00000000.1), *Enterococcus*

*faecalis* (NC_004668.1), *Lactobacillus brevis* (NC_008497.1), and *Lactobacillus plantarum* (NC_004567.2). We used Picard (v.1.109; http://picard.sourceforge.net) to remove duplicate reads and reads with a mapping quality below 20. In addition, we re-aligned sequences flanking indels with GATK (v3.4-46; McKenna *et al.* 2010).

After mapping, we filtered reads due to *D. simulans* contamination, using the method of Bastide *et al*. (2013). To do this, we used fixed differences between *D. simulans* and *D. melanogaster* to identify reads from *D. simulans*. For the nine samples that had a contamination level > 1% (range 1.2 - 8.7%; Table S1), we used custom software to remove reads that mapped preferentially to the *D. simulans* genome (Hu *et al.* 2013) using competitive mapping to references from both species. After applying our decontamination pipeline, contamination levels dropped below 0.4 % for all nine samples.

We used *Qualimap* (v. 2.2., Okonechnikov *et al.* 2016) to evaluate average mapping qualities per population and chromosome, which ranged from 58.3 to 58.8 (Table S1). Sequencing depth ranged from 34x to 115x for autosomes and from 17x to 59x for *X*-chromosomes (Table S1). We then combined individual *bam* files from all samples into a single *mpileup* file using *samtools* (v. 1.3; Li & Durbin 2009). Due to the large number of samples, we implemented quality control criteria for all libraries jointly to call SNPs. To call SNPs, we developed custom software (*PoolSNP*; see Supplementary File 2; available at doi: https://doi.org/10.5061/dryad.rj1gn54) using stringent heuristic parameters: (1) minimum coverage 10x for each sample, (2) maximum coverage < 95th coverage percentile for a given chromosome and sample (to avoid paralogous regions duplicated in the sample but not in the reference), (3) for each allele, a minimum read count > 20x and a minimum read frequency > 0.001, across all samples pooled. These parameters were

optimized based on simulated Pool-Seq data to maximize true positives and minimize false positives (Supplementary File 2). We also excluded SNPs (1) for which more than 20% of all samples did not fulfil the above-mentioned coverage thresholds, (2) which were located within 5 bp of an indel with a minimum count larger than 10x in all samples pooled, and (3) which were located within known TEs based on the *D. melanogaster* TE library v.6.10. We annotated our final set of SNPs with *SNPeff* (v.4.2; Cingolani *et al.* 2012) using the Ensembl genome annotation version BDGP6.82.

**Additional samples**

We obtained genome sequences from African flies from the *Drosophila* Genome Nexus (DGN; http://www.johnpool.net/genomes.html; see Table S5 for SRA accession numbers). We used data from 14 individuals from Rwanda and 40 from Siavonga (Zambia). We mapped these data as described above and built consensus sequences for each haploid sample by only considering alleles with > 0.9 allele frequencies. We converted consensus sequences to *VCF* and used *VCFtools* (Danecek et al. 2011) for downstream analyses.

**Genetic variation in Europe**

We characterized patterns of genetic variation among the 48 samples for the five major chromosomal arms (*X*, *2L*, *2R*, *3L*, *3R*) by estimating $\pi$, Watterson's $\theta$ and Tajima's *D* (Watterson 1975; Nei 1987; Tajima 1989), using corrections for Pool-Seq data (Kofler *et al.* 2011). To perform these analyses for our set of SNPs, we re-implemented the methods of Kofler *et al*. (2011) in Python (PoolGen; doi: https://doi.org/10.5061/dryad.rj1gn54). To calculate unbiased window-wise estimates of parameters, we used an output file of our SNP calling pipeline (*PoolSNP*; doi: https://doi.org/10.5061/dryad.rj1gn54), which indicates for any given site in the reference, if it passed the filtering parameters used for SNP

775 calling. These data allow for the calculation of the effective window-size, which is the
776 difference between the total window-size and the number of sites that did not pass the
777 quality criteria. Using effective windows-sizes as the denominator for the calculation of
778 window-wise averages yields unbiased average estimates. In contrast, dividing the
779 summed statistics in a given window by the total window-size, which is common practice in
780 most software tools, results in an underestimation of averaged parameters. Before
781 calculating the estimators, we subsampled the data to an even coverage of 40x for
782 autosomes and 20x for the *X*-chromosome, as Watterson's $\theta$ and Tajima's *D* are sensitive
783 to coverage variation (Korneliussen *et al.* 2013). We calculated chromosome-wide
784 averages of $\pi$, $\theta$ and Tajima's *D* for autosomes and *X* chromosomes using *R* (R
785 Development Core Team 2009). We tested for correlations between these estimators and
786 latitude, longitude, altitude, and season using a linear regression model: $y_i = Lat + Lon +$
787 $Alt + Season + \varepsilon_i$, where $y_i$ represents $\pi$, $\theta$ or *D*. We used *Lat*, *Lon* and *Alt* as continuous
788 predictors (Table 1) and *Season* as a categorical factor with two levels, corresponding to
789 collection dates before and after 1$^{st}$ September ('summer' and 'fall'), respectively, following
790 Bergland *et al.* (2014) and Kapun *et al.* (2016a). To test for residual spatio-temporal
791 autocorrelation among the samples (Kühn & Dormann 2012), we calculated Moran's *I*
792 (Moran 1950) with the *R* package *spdep* (v.06-15., Bivand & Piras 2015) for the residuals
793 of the above models. For this analysis, we considered samples within 10° latitude /
794 longitude to be neighbours, based on the pairwise geographical distances between
795 collection locations. Whenever these tests revealed significant autocorrelations indicating
796 non-independence, we repeated the above regressions using a spatial weights matrix
797 based on nearest neighbours as described above to test for remaining spatial patterning in
798 residuals as implemented in *spdep*. We also fitted models with run ID as a random factor
799 using the *R* package *lme4* (v.1.1-14; see Supplementary File 2) to test for confounding

effects of variation in error rates among sequencing runs. As these models did not fit significantly better than simpler models, we excluded it from final analysis (see Supplementary File 2 and Table S3).

To investigate genome-wide patterns of variation, we averaged $\pi$, $\theta$, and *D* in 200 kb non-overlapping windows for each sample and chromosomal arm separately and plotted the distributions in *R.* In addition, to investigate fine-scale deviations from neutral expectations, we also calculated Tajima's *D* in 50 kb sliding windows with a step size of 10 kb. We normalized diversity statistics using log-transformation and tested for correlations between $\pi$ and recombination rate for 100 kb non-overlapping windows in *R* and plotted these data using the *ggplot2* (v.2.2.1., Wickham 2016). We used both fine-scale (Comeron *et al.* 2012) and broad-scale (Fiston-Lavier *et al.* 2010) estimates of recombination rate, after converting their coordinates to reference genome v 6.

To identify regions under selection, we used *Pool-hmm* to calculate the SFS (Site Frequency Spectrum) for each sample in the *pileup* format file with the following parameters *–prefix* (to assign a name to each sample), *-n* (number of chromosomes), *--only-spectrum* (for the SFS calculation), *--theta* 0.005 (default), and *-r* 100 (subsampling of 1/100 SNPs). We then split the *pileups* by chromosome and ran *Pool-hmm* with the following parameters: *--prefix*, *-n*, *-k* (per site transition probability between hidden states), *-s* (frequency spectrum file from previous step) and *-e sanger* (*Phred quality* = 33). For the 18 samples for which Tajima's *D* was very low, *Pool-hmm* identified the majority of the genome to be under selection; we thus removed those samples from our analysis. We used three different *k parameters* depending on the sample: $k=1e^{-10}$, $k=1e^{-30}$, and $k=1e^{-40}$ (Table S6A). For windows with significantly low Tajima's D in euchromatic regions, we

identified genes using *bedtools intersect* (v2.27.1) and the *D. melanogaster* v6.12 annotation file from Flybase (Thurmond et al 2019). For genes significant in all populations, we checked whether average Tajima's *D* was among the lowest 10% per chromosome. We tested for enrichment of involvement in particular biological processes using *DAVID* with default parameters (Huang et al 2009).

**Genetic differentiation and population structure in European populations**

To estimate genome-wide pairwise genetic differences, we used custom software to estimate SNP-wise $F_{ST}$ using the approach of Weir and Cockerham (1984) for all pairwise combinations of samples. For each sample, we averaged pairwise $F_{ST}$ between that sample and the other 47 samples and ranked the 48 population samples by overall differentiation.

We inferred demographic patterns by focusing on putatively neutrally evolving SNPs. For this, we used either 4-fold degenerate sites (defined using the genome sequences and the annotation features of the *D. melanogaster* reference genome version 6.12) or short introns (<60 bp; Haddrill *et al.* 2005; Singh *et al.* 2009; Parsch *et al.* 2010; Clemente & Vogl 2012; Lawrie *et al.* 2013). We also restricted our analyses to SNPs that were at least 1 Mb distant from major chromosomal inversions (see below) and those located in genomic regions with high recombination rates (r > 3cM/Mb; Comeron et al. 2012) to minimize the effects of linkage, which may confound analyses of neutral evolution. As the Sheffield (UK) population showed unusually high differentiation from other populations, we repeated the following analyses without the Sheffield sample. To assess isolation by distance (IBD), we averaged pairwise $F_{ST}$ values across all neutral markers. We calculated geographic distance using the haversine formula (Green & Smart 1985), which takes the

spherical curvature of the planet into account. We tested for correlations between linearized genetic differentiation (Slatkin's distance: $F_{ST}/([1-F_{ST}])$ and $\log_{10}$-scaled geographic distance (Slatkin 1985) using Mantel tests implemented in *ade4* (v.1.7-8., Dray & Dufour 2007) with 1,000,000 iterations. In addition, we plotted the 5% smallest and largest $F_{ST}$ values from all 1,128 pairwise comparisons among the 48 population samples onto a map to visualize geographic patterns of genetic differentiation.

We tested for population substructure using two different approaches. First, we performed principal component analysis (PCA) based on unscaled allele frequencies of the neutral marker SNPs, as suggested by Menozzi *et al*. (1978) and Novembre and Stephens (2008), using *LEA* (v. 1.2.0., Frichot *et al.* 2013). We focused on the first three principal components (PCs) and used *mclust* (v. 5.2., Fraley & Raftery 2012) to estimate the number of clusters *via* maximum likelihood and assigned population samples to clusters *via k*-means. In addition, we examined the first three PCs for correlations with latitude, longitude, altitude, and season using general linear models and tested for spatial autocorrelation as above. A Bonferroni-corrected $\alpha$ threshold ($\alpha' = 0.05/3 = 0.017$) was used to correct for multiple testing.

In a second, complementary approach, we inferred population delineation using model-based clustering as implemented in *ConStruct* (v.1.0.2; Bradburd *et al.* 2018). In contrast to most clustering-based methods, *ConStruct* incorporates continuous isolation by distance to avoid inflating estimates of the number of clusters and allows estimating admixture among populations. We ran spatial models with three MCMC chains per run and 10,000 iterations and compared the goodness of fit for models incorporating 1 to 10 spatial layers by cross-validation.

875

876 **Mitochondrial DNA**

877 To obtain consensus mitochondrial sequences for each of the 48 European populations,
878 we aligned reads from individual FASTQ files and replaced minor variants with the major
879 variant using *Coral* (Salmela & Schröder 2011). This method prevents ambiguities from
880 interfering with the assembly process. We assembled a genome for each population from
881 the modified FASTQ files using *SPAdes* with standard parameters and *k*-mers of size 21,
882 33, 55, and 77 (Bankevich *et al.* 2012). Mitochondrial contigs were retrieved by *blastn*,
883 using the *D. melanogaster* NC 024511 sequence as a query and each genome assembly
884 as the database. To avoid nuclear mitochondrial DNA segments (numts), we ensured that
885 only contigs with a higher than average coverage of the genome were retrieved. When
886 multiple contigs were available for the same region, the one with the highest coverage was
887 selected. Possible contamination with *D. simulans* was assessed by looking for two or
888 more consecutive sites that show the same variant as *D. simulans* and looking for
889 alternative contigs for that region with similar coverage. As an additional quality control
890 measure, we also examined the presence of pairs of sites showing four gametic types
891 using *DNAsp* 6 (Rozas *et al.* 2017) – given that there is no recombination in mitochondrial
892 DNA no such sites are expected. The very few sites presenting such features were
893 rechecked by looking for alternative contigs for that region and were corrected if needed.
894 The uncorrected raw reads for each population were mapped on top of the different
895 consensus haplotypes using *Express* as implemented in *Trinity* (Grabherr *et al.* 2011). If
896 most reads for a given population mapped to the consensus sequence derived for that
897 population the consensus sequence was retained, otherwise it was discarded as a
898 possible chimera between different mitochondrial haplotypes. The repetitive mitochondrial
899 hypervariable region is difficult to assemble and was therefore not used; the mitochondrial

region was thus analysed as in Cooper *et al*. (2015). Mitochondrial genealogy was estimated using statistical parsimony (TCS network; Clement *et al.* 2000), as implemented in *PopArt* (http://popart.otago.ac.nz), and the surviving mitochondrial haplotypes. Frequencies of the different mitochondrial haplotypes were estimated from FPKM values using the surviving mitochondrial haplotypes and expressed as implemented in *Trinity* (Grabherr *et al.* 2011).

**Transposable elements**

To quantify transposable element (TE) abundance in each sample, we assembled and quantified repeats from unassembled sequenced reads using *dnaPipeTE* (v.1.2., Goubert *et al.* 2015). Only the left read of each pair were used. As the vast majority of high-quality trimmed reads were longer than 135 bp, we discarded reads shorter than this before sampling. Reads matching mtDNA were filtered out by mapping to the *D. melanogaster* reference mitochondrial genome (NC_024511.2. 1) with *bowtie2* (v. 2.1.0., Langmead & Salzberg 2012). Prokaryotic sequences, including reads from symbiotic bacteria such as *Wolbachia*, were filtered out from the reads using the implementation of *blastx vs.* the non-redundant protein database (nr) using *DIAMOND* (v. 0.8.7, Buchfink *et al.* 2015). To quantify TE content, we subsampled a proportion of the raw reads (after filtering) corresponding to a genome coverage of 0.1X (assuming a genome size of 175 MB), and then assembled these reads with *Trinity* (Grabherr *et al.* 2011). Due to the low coverage of the genome obtained with the subsampled reads, only repetitive DNA present in multiple copies should be fully assembled (Goubert *et al.* 2015). To assess the constancy of the estimates, we repeated this process with three iterations per sample, as recommended by the program guidelines.

We further estimated frequencies of TEs present in the reference genome with *T-lex2* (v. 2.2.2., Fiston-Lavier *et al.* 2015), using all annotated TEs (5,416 TEs) in version 6.04 of the *D. melanogaster* genome from flybase.org (Gramates *et al.* 2017). For 108 of these TEs, we used the corrected coordinates as described in Fiston-Lavier *et al*. (2015), based on the identification of target site duplications at the site of the insertion. We excluded TEs nested or flanked by other TEs (<100 bp on each side of the TE), and TEs, which are part of segmental duplications, since *T-lex2* does not provide accurate frequency estimates in complex regions (Fiston-Lavier *et al.* 2015). We additionally excluded the INE-1 TE family, as this TE family is ancient, with 2,234 insertions in the reference genome, which appear to be mostly fixed (Kapitonov & Jurka 2003). After applying these filters, we were able to estimate frequencies of 1,630 TE insertions from 113 families from the three main orders, LTR, non-LTR, and DNA across all *DrosEU* samples. Because the mapper used by *T-lex2* to detect the presence of insertions (presence module) only accepts reads ≤127 bp, we trimmed reads longer than 100 bp into two equally sized fragments using *Trimmomatic* (v. 0.35; Bolger *et al.* 2014) with the CROP and HEADCROP parameters.

To avoid inaccurate TE frequency estimates due to very low numbers of reads, we only considered frequency estimates based on at least 3 reads. Despite the stringency of *T-lex2* to select only high-quality reads, we additionally discarded frequency estimates supported by more than 90 reads, i.e. 3 times the average coverage of the sample with the lowest coverage (CH_Cha_14_43, Table S1), in order to avoid non-uniquely mapping reads. This filtering allows to estimate TE frequencies for ~96% (92.9% to 97.8%) of the TEs in each population. For 85% of the TEs, we were able to estimate their frequencies in more than 44 out of 48 *DrosEU* samples.

We tested for correlations between TE insertion frequencies and recombination rates using Spearman's rank correlations as implemented in *R*. For SNPs, we used

recombination rates from Comeron *et al*. (2012) and from Fiston-Lavier *et al.* (2010) in non-overlapping 100 kb windows and assigned to each TE insertion the recombination rate of the corresponding window.

To test for spatio-temporal variation of TE insertions, we excluded TEs with an interquartile range (IQR) < 10. We tested the population frequencies of the remaining 141 insertions for correlations with latitude, longitude, altitude, and season using generalized linear models (ANCOVA) following the method used for SNPs but with a binomial error structure in *R*. We further tested if significant correlations with either of the predictor variables deviated from expectations under neutral evolution. To this end, we repeated the ANCOVA analyses on 8,727 presumably neutrally evolving 4-fold degenerate sites that we described previously in the demographic analyses. Based on *F*-ratios obtained from the ANCOVA models for each neutral SNP and predictor, we built empirical density functions and calculated empirical *p*-values for each TE by integrating over the area of the curve that is delineated by the *F*-value specific for the given TE and the maximum *F*-ratio in the neutral dataset.

We also tested for residual spatio-temporal autocorrelations in TE insertion frequencies, with Moran's *I* test (Moran 1950; Kühn & Dormann 2012). We used Bonferroni corrections to account for multiple testing ($\alpha$'= 0.05/141 = 0.00035) and only considered Bonferroni-corrected p-values < 0.001 to be significant. To test TE family enrichment among the significant TEs we performed a $\chi^2$ test and applied Yate's correction to account for the low number of some of the cells.

**Inversion polymorphisms**

Since Pool-Seq data precludes a direct assessment of the presence and frequencies of chromosomal inversions, we indirectly estimated inversion frequencies using a panel of

approximately 400 inversion-specific marker SNPs (Kapun *et al.* 2014) for six cosmopolitan inversions (*In(2L)t, In(2R)NS, In(3L)P, In(3R)C, In(3R)Mo, In(3R)Payne*). We averaged allele frequencies of these markers in each sample separately. To test for clinal variation in the frequencies of inversions, we tested for correlations with latitude, longitude, altitude and season using generalized linear models with a binomial error structure in *R* to account for the biallelic nature of karyotype frequencies. In addition, we Bonferroni-corrected the *α* threshold (*α*'= 0.05/7 = 0.007) to account for multiple testing, accounted for residual spatio-temporal autocorrelations and tested if *F*-ratios of the ANCOVAs deviated from neutral expectations as explained above.

**Microbiome**

Raw sequences were trimmed, and quality filtered as described for the genomic data analysis. The remaining high-quality sequences were mapped against the *D. melanogaster* genome (v.6.04) including mitochondria using *bbmap* (v. 35; Bushnell 2016) with standard settings. The unmapped sequences were submitted to the online classification tool, *MGRAST* (Meyer *et al.* 2008) for annotation. Taxonomy information was downloaded and analysed in *R* (v. 3.2.3; R Development Core Team 2009) using the *matR* (v. 0.9; Braithwaite & Keegan) and RJSONIO (v. 1.3; Lang) packages. Metazoan sequence features were removed. For microbial load comparisons, the number of protein features identified by *MGRAST* for each taxon and sample was divided by the number of sequences that mapped to *D. melanogaster* chromosomes *X*, *Y, 2L*, *2R*, *3L*, *3R* and *4*.

We also surveyed the datasets for the presence of novel DNA viruses by performing *de novo* assembly of the non-fly reads using *SPAdes* 3.9.0 (Bankevich *et al.* 2012) and using conceptual translations to query virus proteins from *Genbank* using *DIAMOND* '*blastp*'

(Buchfink *et al.* 2015). In three cases (*Kallithea* virus, *Vesanto* virus, *Viltain* virus), reads from a single sample pool were sufficient to assemble a (near) complete genome. In two other cases, fragmentary assemblies allowed us to identify additional publicly available datasets that contained sufficient reads to complete the genomes (*Linvill Road* virus, *Esparto* virus; completed using SRA datasets SRR2396966 and SRR3939042, respectively). Novel viruses were provisionally named based on the localities where they were first detected, and the corresponding novel genome sequences were submitted to Genbank (KX130344, KY608910, KY457233, KX648533-KX648536). To assess the relative amount of viral DNA, unmapped (non-fly) reads from each sample pool were mapped to repeat-masked *Drosophila* DNA virus genomes using *bowtie2*, and coverage normalized relative to virus genome length and the number of mapped *Drosophila* reads.

## Acknowledgments

We are grateful to all members of the *DrosEU* and Dros-RTEC consortia and to Dmitri Petrov (Stanford University) for support and discussion. *DrosEU* is funded by a Special Topic Networks (STN) grant from the European Society for Evolutionary Biology (ESEB). Computational analyses were partially executed at the Vital-IT bioinformatics facility of the University of Lausanne (Switzerland), at the computing facilities of the CC LBBE/PRABI in Lyon (France) and at the bwUniCluster of the state of Baden-Württemberg (bwHPC).

## Additional information

### Funding


| Funder | Grant reference number | Author |
|---|---|---|

| | | |
|---|---|---|
| University of Freiburg Research Innovation Fund 2014. Deutsche Forschungsgemeinschaft | STA1154/4-1Project 408908608 | Fabian Staubach |
| Academy of Finland | #268241 | Maaria Kankare |
| Academy of Finland | #272927 | Maaria Kankare |
| Russian Foundation of Basic Research | #15-54-46009 CT_a | Elena G. Pasyukova |
| Danish Natural Science Research Council | 4002-00113 | Volker Loeschcke |
| Ministerio de Economia y Competitividad | CTM2017-88080 (AEI/FEDER, UE) | Marta Pascual |
| CNRS | UMR 9191 | Catherine Montchamp-Moreau |
| Vetenskapsrådet | 2011-05679 | Jessica Abbott |
| Vetenskapsrådet | 2015-04680 | Jessica Abbott |
| Emmy Noether Programme of the Deutsche Forschungsgemeinschaft, DFG | PO 1648/3-1 | Nico Posnien |
| National Institute of Health (NIH) | R35GM119686 | Alan O. Bergland |
| Ministerio de Economia y Competitividad | CGL2013-42432-P | Maria Pilar Garcia Guerreiro |
| Scientific and Technological Research Council of Turkey (TUBITAK) | #214Z238 | Banu Sebnem Onder |
| ANR Exhyb | 14-CE19-0016 | Cristina Vieira |

| | | |
|---|---|---|
| Network of Excellence LifeSpan | FP6 036894 | Bas J. Zwaan |
| IDEAL | FP7/2007-2011/259679 | Bas J. Zwaan |
| Israel Science Foundation | 1737/17 | Eran Tauber |
| National Institute of Health (NIH) | R01GM100366 | Paul S. Schmidt |
| Deutsche Forschungsgemeinschaft | PA 903/8-1 | John Parsch |
| Austrian Science Fund (FWF) | P27048 | Andrea J. Betancourt |
| Biotechnology and Biological Sciences Research Council (BBSRC) | BB/P00685X/1 | Andrea J. Betancourt |
| Swiss National Science Foundation (SNSF) | PP00P3_133641 | Thomas Flatt |
| Swiss National Science Foundation (SNSF) | PP00P3_165836 | Thomas Flatt |
| European Comission | H2020-ERC-2014CoG-647900 | Josefa González |
| Secretaria d'Universitats i Recerca. Dept Economia i Coneixement. Generalitat de Catalunya | GRC 2017 SGR 880 | Josefa González |
| Ministerio de Economia y Competitividad | FEDER BFU2014-57779-P | Josefa González |


## Author contributions

Martin Kapun, Visualization, Writing-original draft preparation, Formal analysis, Conceptualization, Writing-review & editing, Supervision, Methodology, Investigation, Data curation, Project administration, Validation, Resources, Software; Maite G. Barrón,

Visualization, Writing-original draft preparation, Formal analysis, Conceptualization, Writing-review & editing, Methodology, Investigation, Data curation, Project administration, Validation, Resources, Software; Fabian Staubach, Visualization, Writing-original draft preparation, Formal analysis, Conceptualization, Writing-review & editing, Supervision, Funding acquisition, Methodology, Investigation, Data curation, Validation, Resources, Software; Jorge Vieira, Visualization, Writing-original draft preparation, Formal analysis, Conceptualization, Writing-review & editing, Methodology, Investigation, Validation, Resources; Darren J. Obbard, Writing-original draft preparation, Formal analysis, Conceptualization, Writing-review & editing, Methodology, Investigation, Validation, Resources; Clément Goubert, Visualization, Writing-original draft preparation, Formal analysis, Conceptualization, Writing-review & editing, Investigation, Resources; Omar Rota-Stabelli, Visualization, Writing-original draft preparation, Formal analysis, Conceptualization, Writing-review & editing, Methodology, Investigation, Resources; Maaria Kankare, Writing-original draft preparation, Conceptualization, Writing-review & editing, Methodology, Investigation, Resources; María Bogaerts-Márques, Alejandro Sánchez-Gracia, Formal analysis, Writing-review & editing, Investigation, Validation, Resources; Annabelle Haudry, Writing-original draft preparation, Formal analysis, Conceptualization, Writing-review & editing, Investigation, Validation, Resources; R. Axel W. Wiberg, Writing-original draft preparation, Formal analysis, Conceptualization, Writing-review & editing, Methodology, Investigation, Resources, Software; Lena Waidele, Svitlana Serga, Patricia Gibert, Damiano Porcelli, Sonja Grath, Eliza Argyridou, Lain Guio, Mads Fristrup Schou, Conceptualization, Writing-review & editing, Investigation, Resources; Iryna Kozeretska, Conceptualization, Writing-review & editing, Methodology, Investigation, Resources; Elena G. Pasyukova, Marta Pascual, Alan O. Bergland, Conceptualization, Writing-review & editing, Funding acquisition, Methodology, Investigation, Resources;

Volker Loeschcke, Catherine Montchamp-Moreau, Jessica Abbott, Nico Posnien, Maria Pilar Garcia Guerreiro, Banu Sebnem Onder, Conceptualization, Writing-review & editing, Funding acquisition, Investigation, Resources; Cristina P. Vieira, Visualization, Formal analysis, Conceptualization, Writing-review & editing, Investigation, Resources; Élio Sucena, Conceptualization, Writing-review & editing, Methodology, Investigation, Project administration, Resources; Cristina Vieira, Michael G. Ritchie, Thomas Flatt, Josefa González, Writing-original draft preparation, Conceptualization, Writing-review & editing, Supervision, Funding acquisition, Methodology, Investigation, Project administration, Validation, Resources; Bart Deplancke, Conceptualization, Writing-review & editing, Funding acquisition, Investigation; Bas J. Zwaan, Visualization, Writing-original draft preparation, Conceptualization, Writing-review & editing, Supervision, Funding acquisition, Methodology, Investigation, Project administration; Eran Tauber, Writing-original draft preparation, Conceptualization, Writing-review & editing, Funding acquisition, Methodology, Investigation, Resources; Dorcas J. Orengo, Eva Puerma, Conceptualization, Writing-review & editing, Investigation, Validation, Resources; Montserrat Aguadé, Writing-original draft preparation, Conceptualization, Writing-review & editing, Methodology, Investigation, Validation, Resources; Paul S. Schmidt, John Parsch, Writing-original draft preparation, Conceptualization, Writing-review & editing, Funding acquisition, Methodology, Investigation, Validation, Resources; Andrea J. Betancourt, Writing-original draft preparation, Formal analysis, Conceptualization, Writing-review & editing, Supervision, Funding acquisition, Methodology, Investigation, Project administration, Validation, Resources.

**Author ORCIDs**

| Names | ORCID |
|---|---|
| Martin Kapun | 0000-0002-3810-0504 |
| Maite G. Barrón | 0000-0001-6146-6259 |
| Fabian Staubach | 0000-0002-8097-2349 |
| Jorge Vieira | 0000-0001-7032-5220 |
| Darren J. Obbard | 0000-0001-5392-8142 |
| Clément Goubert | 0000-0001-8034-5559 |
| Omar Rota-Stabelli | 0000-0002-0030-7788 |
| Maaria Kankare | 0000-0003-1541-9050 |
| María Bogaerts-Márquez | 0000-0001-9107-984X |
| Annabelle Haudry | 0000-0001-6088-0909 |
| R. Axel W. Wiberg | 0000-0002-8074-8670 |
| Lena Waidele | 0000-0002-6323-6438 |
| Iryna Kozeretska | 0000-0002-6485-1408 |
| Elena G. Pasyukova | 0000-0002-6491-8561 |
| Volker Loeschcke | 0000-0003-1450-0754 |
| Marta Pascual | 0000-0002-6189-0612 |
| Cristina P. Vieira | 0000-0002-7139-2107 |
| Svitlana Serga | 0000-0003-1875-3185 |
| Catherine Montchamp-Moreau | 0000-0002-5044-9709 |
| Jessica Abbott | 0000-0002-8743-2089 |
| Patricia Gibert | 0000-0002-9461-6820 |
| Damiano Porcelli | 0000-0002-9019-5758 |
| Nico Posnien | 0000-0003-0700-5595 |

| | |
|---|---|
| Alejandro Sánchez-Gracia | 0000-0003-4543-4577 |
| Sonja Grath | 0000-0003-3621-736X |
| Élio Sucena | 0000-0001-8810-870X |
| Alan O. Bergland | 0000-0001-7145-7575 |
| Maria Pilar Garcia Guerreiro | 000-0001-9951-1879X |
| Banu Sebnem Onder | 0000-0002-3003-248X |
| Eliza Argyridou | 0000-0002-6890-4642 |
| Lain Guio | 0000-0002-5481-5200 |
| Mads Fristrup Schou | 0000-0001-5521-5269 |
| Bart Deplancke | 0000-0001-9935-843X |
| Cristina Vieira | 0000-0003-3414-3993 |
| Michael G. Ritchie | 0000-0001-7913-8675 |
| Bas J. Zwaan | 0000-0002-8221-4998 |
| Eran Tauber | 0000-0003-4018-6535 |
| Dorcas J. Orengo | 0000-0001-7911-3224 |
| Eva Puerma | 0000-0001-7261-187X |
| Montserrat Aguadé | 0000-0002-3884-7800 |
| Paul S. Schmidt | 0000-0002-8076-6705 |
| John Parsch | 0000-0001-9068-5549 |
| Andrea J. Betancourt | 0000-0001-9351-1413 |
| Thomas Flatt | 0000-0002-5990-1503 |
| Josefa González | 0000-0001-9824-027X |


## References

1078 Adrian AB, Comeron JM (2013) The *Drosophila* early ovarian transcriptome provides
1079 insight to the molecular causes of recombination rate variation across genomes. *BMC*
1080 *Genomics*, **14**, 1-12.
1081 Adrion JR, Hahn MW, Cooper BS (2015) Revisiting classic clines in *Drosophila*
1082 *melanogaster* in the age of genomics. *Trends in Genetics*, **31**, 434–444.
1083 Alonso-Blanco C, Andrade J, Becker C *et al.* (2016) 1,135 Genomes Reveal the Global
1084 Pattern of Polymorphism in *Arabidopsis thaliana*. *Cell,* **166**, 481–491.
1085 Anderson AR, Hoffmann AA, McKechnie SW, Umina PA, Weeks AR (2005) The latitudinal
1086 cline in the *In(3R)Payne* inversion polymorphism has shifted in the last 20 years in
1087 Australian *Drosophila melanogaster* populations. *Molecular Ecology,* **14**, 851–858.
1088 Andolfatto P (2001) Contrasting Patterns of *X*-Linked and Autosomal Nucleotide Variation
1089 in *Drosophila melanogaster* and *Drosophila simulans*. *Molecular Biology and Evolution*,
1090 **18**, 279–290.
1091 Arguello JR, Laurent S, Clark AG. 2019. Demographic History of the Human Commensal
1092 *Drosophila melanogaster*. *Genome Biology and Evolution* **11**:844–854.
1093 Aulard S, David JR, Lemeunier F (2002) Chromosomal inversion polymorphism in
1094 Afrotropical populations of *Drosophila melanogaster*. *Genetic Research*, **79**, 49–63.
1095 Auton A, Abecasis GR, Altshuler DM (2015) A global reference for human genetic
1096 variation. *Nature*, **526**, 68–74.
1097 Bankevich A, Nurk S, Antipov D *et al.* (2012) *SPAdes, a New Genome Assembly*
1098 *Algorithm and Its Applications to Single-cell Sequencing (7th Annual SFAF Meeting,*
1099 *2012).* Mary Ann Liebert Inc.
1100 Barata A, Santos SC, Malfeito-Ferreira M, Loureiro V (2012) New insights into the
1101 ecological interaction between grape berry microorganisms and *Drosophila* flies during
1102 the development of sour rot. *Microbial Ecology*, **64**, 416–430.

1103 Bartolomé C, Maside X, Charlesworth B (2002) On the Abundance and Distribution of
1104 Transposable Elements in the Genome of *Drosophila melanogaster*. *Molecular Biology*
1105 *and Evolution*, **19**, 926–937.
1106 Bastide H, Betancourt A, Nolte V *et al.* (2013) A genome-wide, fine-scale map of natural
1107 pigmentation variation in *Drosophila melanogaster*. *PLoS Genetics*, **9**, e1003534.
1108 Baudry E, Viginier B, Veuille M (2004) Non-African populations of *Drosophila*
1109 *melanogaster* have a unique origin. *Molecular Biology and Evolution*, **21**, 1482–1491.
1110 Becher PG, Flick G, Rozpędowska E *et al.* (2012) Yeast, not fruit volatiles mediate
1111 *Drosophila melanogaster* attraction, oviposition and development. *Functional Ecology*,
1112 **26**, 822–828.
1113 Begun DJ, Aquadro CF (1992) Levels of naturally occurring DNA polymorphism correlate
1114 with recombination rates in *D. melanogaster*. *Nature*, **356**, 519–520.
1115 Begun DJ, Aquadro CF (1993) African and North American populations of *Drosophila*
1116 *melanogaster* are very different at the DNA level. *Nature*, **365**, 548–550.
1117 Begun DJ, Holloway AK, Stevens K *et al.* (2007) Population Genomics: Whole-Genome
1118 Analysis of Polymorphism and Divergence in *Drosophila simulans*. *PLoS Biology*, **5**,
1119 e310.
1120 Behrman EL, Howick VM, Kapun M *et al.* (2018) Rapid seasonal evolution in innate
1121 immunity of wild *Drosophila melanogaster*. *Proceedings of the Royal Society of*
1122 *London B*, **285**, 20172599.
1123 Beisswanger S, Stephan W, De Lorenzo D (2006) Evidence for a Selective Sweep in the
1124 *wapl* Region of *Drosophila melanogaster*. *Genetics*, **172**, 265–274.
1125 Bergland AO, Behrman EL, O'Brien KR, Schmidt PS, Petrov DA (2014) Genomic Evidence
1126 of Rapid and Stable Adaptive Oscillations over Seasonal Time Scales in *Drosophila*.
1127 *PLoS Genetics*, **10**, e1004775.

1128 Bergland AO, Tobler R, González J, Schmidt P, Petrov D (2016) Secondary contact and
1129 local adaptation contribute to genome-wide patterns of clinal variation in *Drosophila*
1130 melanogaster. *Molecular Ecology*, **25**, 1157–1174.
1131 Betancourt AJ, Kim Y, Orr HA (2004) A pseudohitchhiking model of X vs. autosomal
1132 diversity. *Genetics*, **168**, 2261–2269.
1133 Betancourt AJ, Welch JJ, Charlesworth B (2009) Reduced effectiveness of selection
1134 caused by a lack of recombination. *Current Biology*, **19**, 655–660.
1135 Bilder D, Irvine KD (2017) Taking Stock of the *Drosophila* Research Ecosystem. *Genetics*
1136 **206**, 1227–1236
1137 Bivand R, Piras G (2015) Comparing Implementations of Estimation Methods for Spatial
1138 Econometrics. *Journal of Statistical Software*, **63**, 1–36.
1139 Black WC IV, Black WC IV, Baer CF, Antolin MF, DuTeau NM (2001) Population
1140 genomics: genome-wide sampling of insect populations. *Annual Review of*
1141 *Entomology*, **46,** 441–469
1142 Blumenstiel JP, Chen X, He M, Bergman CM (2014) An Age-of-Allele Test of Neutrality for
1143 Transposable Element Insertions. *Genetics*, **196**, 523–538.
1144 Boitard S, Schlötterer C, Nolte V, Pandey RV, Futschik A (2012) Detecting Selective
1145 Sweeps from Pooled Next-Generation Sequencing Samples. *Molecular Biology and*
1146 *Evolution*, **29**, 2177–2186.
1147 Boitard S, Kofler R, Françoise P, Robelin D, Schlötterer C, Futschik A (2013) Pool-hmm: a
1148 Python program for estimating the allele frequency spectrum and detecting selective
1149 sweeps from next generation sequencing of pooled samples. *Mol Ecol Resour,* **13**,
1150 337–340.
1151 Bolger AM, Lohse M, Usadel B (2014) Trimmomatic: a flexible trimmer for Illumina
1152 sequence data. *Bioinformatics*, **30**, 2114–2120.

1153 Boussy IA, Itoh M, Rand D, Woodruff RC (1998) Origin and decay of the P element-
1154 associated latitudinal cline in Australian *Drosophila melanogaster*. *Genetica*, **104**, 45–
1155 57.
1156 Božičević V, Hutter S, Stephan W, Wollstein A (2016) Population genetic evidence for cold
1157 adaptation in European *Drosophila melanogaster* populations. *Molecular Ecology*, **25**,
1158 1175–1191.
1159 Bradburd GS, Coop GM, Ralph PL (2018) Inferring Continuous and Discrete Population
1160 Genetic Structure Across Space. *Genetics* **210**, 33–52.
1161 Braithwaite DP, Keegan KP *matR: Metagenomics Analysis Tools for R*. https://CRAN.R-
1162 project.org/package=matR.
1163 Buchfink B, Xie C, Huson DH (2015) Fast and sensitive protein alignment using
1164 DIAMOND. *Nature Methods*, **12**, 59–60.
1165 Buser CC, Newcomb RD, Gaskett AC, Goddard MR (2014) Niche construction initiates the
1166 evolution of mutualistic interactions. *Ecology Letters*, **17**, 1257–1264.
1167 Bushnell B (2016) *BBMap short read aligner*. URL http://sourceforge. net/projects/bbmap.
1168 Caracristi G, Schlötterer C (2003) Genetic Differentiation Between American and
1169 European *Drosophila melanogaster* Populations Could Be Attributed to Admixture of
1170 African Alleles. *Molecular Biology and Evolution*, **20**, 792–799.
1171 Casillas S, Barbadilla A (2017) Molecular Population Genetics. *Genetics*, **205**, 1003–1035.
1172 Catania F, Kauer MO, Daborn PJ *et al.* (2004) World-wide survey of an Accord insertion
1173 and its association with DDT resistance in *Drosophila melanogaster. Molecular*
1174 *Ecology*, **13**, 2491–2504.
1175 Cavalli-Sforza LL (1966) Population Structure and Human Evolution. *Proceedings of the*
1176 *Royal Society of London B*, **164**, 362–379.

1177 Chandler JA, James PM (2013) Discovery of trypanosomatid parasites in globally
1178 distributed *Drosophila* species. *PLoS ONE*, **8**, e61937.
1179 Chandler JA, Eisen JA, Kopp A (2012) Yeast communities of diverse *Drosophila* species:
1180 comparison of two symbiont groups in the same hosts. *Applied and Environmental*
1181 *Microbiology*, **78**, 7327–7336.
1182 Chandler JA, Lang JM, Bhatnagar S, Eisen JA, Kopp A (2011) Bacterial communities of
1183 diverse *Drosophila* species: ecological context of a host-microbe model system. *PLoS*
1184 *Genetics*, **7**, e1002272.
1185 Charlesworth B (2001) The effect of life-history and mode of inheritance on neutral genetic
1186 variability. *Genetical Research* **77**, 153–166.
1187 Charlesworth B, Sniegowski P, Stephan W (1994) The evolutionary dynamics of repetitive
1188 DNA in eukaryotes. *Nature*, **371**, 215–220.
1189 Cheng C, White BJ, Kamdem C *et al.* (2012) Ecological genomics of *Anopheles gambiae*
1190 along a latitudinal cline: a population-resequencing approach. *Genetics*, **190**, 1417–
1191 1432.
1192 Cingolani P, Platts A, Wang LL *et al.* (2012) A program for annotating and predicting the
1193 effects of single nucleotide polymorphisms, SnpEff: SNPs in the genome of *Drosophila*
1194 *melanogaster* strain $w^{1118}$; *iso-2*; *iso-3*. *Fly (Austin)*, **6**, 80–92.
1195 Clement M, Posada D, Crandall KA (2000) TCS: a computer program to estimate gene
1196 genealogies. *Molecular Ecology*, **9**, 1657–1659.
1197 Clemente F, Vogl C (2012) Unconstrained evolution in short introns? – An analysis of
1198 genome-wide polymorphism and divergence data from *Drosophila*. *Journal of*
1199 *Evolutionary Biology*, **25**, 1975–1990.
1200 Comeron JM, Ratnappan R, Bailin S (2012) The many landscapes of recombination in
1201 *Drosophila melanogaster*. *PLoS Genetics*, **8**, e1002905.

1202 Cooper BS, Burrus CR, Ji C, Hahn MW, Montooth KL (2015) Similar Efficacies of
1203 Selection Shape Mitochondrial and Nuclear Genes in Both *Drosophila melanogaster*
1204 and *Homo sapiens*. *G3*, **5**, 2165–2176.
1205 Corbett-Detig RB, Hartl DL (2012) Population Genomics of Inversion Polymorphisms in
1206 *Drosophila melanogaster*. *PLoS Genetics*, **8**, e1003056.
1207 Cridland JM, Macdonald SJ, Long AD, Thornton KR (2013) Abundance and distribution of
1208 transposable elements in two *Drosophila* QTL mapping resources. *Molecular Biology*
1209 *and Evolution*, **30**, 2311–2327.
1210 Daborn PJ, Yen JL, Bogwitz MR *et al.* (2002) A single p450 allele associated with
1211 insecticide resistance in *Drosophila*. *Science*, **297**, 2253–2256.
1212 David JR, Capy P (1988) Genetic variation of *Drosophila melanogaster* natural
1213 populations. *Trends in Genetics*, **4**, 106–111.
1214 de Jong G, Bochdanovits Z (2003) Latitudinal clines in *Drosophila melanogaster*: body
1215 size, allozyme frequencies, inversion frequencies, and the insulin-signalling pathway.
1216 *Journal of Genetics*, **82**, 207–223.
1217 Dieringer D, Nolte V, Schlötterer C (2005) Population structure in African *Drosophila*
1218 *melanogaster* revealed by microsatellite analysis. *Molecular Ecology*, **14**, 563–573.
1219 Dobzhansky T (1970) *Genetics of the Evolutionary Process*. Columbia University Press.
1220 Dray S, Dufour A-B (2007) The ade4 Package: Implementing the Duality Diagram for
1221 Ecologists. *Journal of Statistical Software*, **22**. 1–20
1222 Duchen P, Zivkovic D, Hutter S, Stephan W, Laurent S (2013) Demographic inference
1223 reveals African and European admixture in the North American *Drosophila*
1224 *melanogaster* population. *Genetics*, **193**, 291–301.

1225 Durmaz E, Benson C, Kapun M, Schmidt P, Flatt T (2018) An Inversion Supergene in
1226 *Drosophila* Underpins Latitudinal Clines in Survival Traits. *Journal of Evolutionary*
1227 *Biology*, in press.
1228 Ellegren H (2014) Genome sequencing and population genomics in non-model organisms.
1229 *Trends in Ecology & Evolution*, **29**, 51–63.
1230 Elya C, Lok TC, Spencer QE, McCausland H, Martinez CC, Eisen MB (2018) Robust
1231 manipulation of the behavior of *Drosophila melanogaster* by a fungal pathogen in the
1232 laboratory, *eLife, **7**,* e34414
1233 Fabian DK, Kapun M, Nolte V *et al.* (2012) Genome-wide patterns of latitudinal
1234 differentiation among populations of *Drosophila melanogaster* from North America.
1235 *Molecular Ecology*, **21**, 4748–4769.
1236 Fabian DK, Lack JB, Mathur V *et al.* (2015) Spatially varying selection shapes life history
1237 clines among populations of *Drosophila melanogaster* from sub-Saharan Africa.
1238 *Journal of Evolutionary Biology*, **28**, 826–840.
1239 Fiston-Lavier A-S, Barrón MG, Petrov DA, González J (2015) T-lex2: genotyping,
1240 frequency estimation and re-annotation of transposable elements using single or
1241 pooled next-generation sequencing data. *Nucleic Acids Research*, **43**, e22–e22.
1242 Fiston-Lavier A-S, Singh ND, Lipatov M, Petrov DA (2010) *Drosophila melanogaster*
1243 recombination rate calculator. *Gene*, **463**, 18–20.
1244 Fraley C, Raftery AE (2012) *mclust Version 4 for R: Normal Mixture Modeling for Model-*
1245 *Based Clustering, Classification, and Density Estimation*. https://cran.r-
1246 project.org/web/packages/mclust
1247 Francalacci P, Sanna D (2008) History and geography of human Y-chromosome in
1248 Europe: a SNP perspective. *Journal of Anthropological Sciences*, **86**, 59–89.

1249 Frichot E, Schoville SD, Bouchard G, François O (2013) Testing for associations between
1250 loci and environmental gradients using latent factor mixed models. *Molecular Biology*
1251 *and Evolution*, **30**, 1687–1699.
1252 Futschik A (2010) The next generation of molecular markers from massively parallel
1253 sequencing of pooled DNA samples. *Genetics*, **186**, 207–218.
1254 González J, Karasov TL, Messer PW, Petrov DA (2010) Genome-Wide Patterns of
1255 Adaptation to Temperate Environments Associated with Transposable Elements in
1256 *Drosophila*. *PLoS Genetics*, **6**, e1000905.
1257 González J, Lenkov K, Lipatov M, Macpherson JM, Petrov DA (2008) High Rate of Recent
1258 Transposable Element–Induced Adaptation in *Drosophila melanogaster*. *PLoS Biology*,
1259 **6**, e251.
1260 Goubert C, Modolo L, Vieira C *et al.* (2015) De Novo Assembly and Annotation of the
1261 Asian Tiger Mosquito (*Aedes albopictus*) Repeatome with dnaPipeTE from Raw
1262 Genomic Reads and Comparative Analysis with the Yellow Fever Mosquito (*Aedes*
1263 *aegypti*). *Genome Biology and Evolution*, **7**, 1192–1205.
1264 Grabherr MG, Haas BJ, Yassour M *et al.* (2011) Full-length transcriptome assembly from
1265 RNA-Seq data without a reference genome. *Nature Biotechnology*, **29**, 644–652.
1266 Gramates LS, Marygold SJ, Santos GD *et al.* (2017) FlyBase at 25: looking to the future.
1267 *Nucleic Acids Research*, **45**, D663–D671.
1268 Green RM, Smart WM (1985) *Textbook on Spherical Astronomy*. Cambridge University.
1269 Grenier JK, Arguello JR, Moreira MC *et al.* (2015) Global Diversity Lines-A Five-Continent
1270 Reference Panel of Sequenced *Drosophila melanogaster* Strains. *G3*, **5**, 593–603.
1271 Guirao-Rico S, González J (2019) Evolutionary insights from large scale resequencing
1272 datasets in Drosophila melanogaster. *Current Opinion in Insect Science*, Insect
1273 genomics • Development and regulation **31**, 70–76.

1274 Haddrill PR, Charlesworth B, Halligan DL, Andolfatto P (2005) Patterns of intron sequence
1275 evolution in *Drosophila* are dependent upon length and GC content. *Genome Biology*,
1276 **6**, R67.
1277 Hales KG, Korey CA, Larracuente AM, Roberts DM (2015) Genetics on the Fly: A Primer
1278 on the *Drosophila* Model System. *Genetics*, **201**, 815–842.
1279 Hamilton PT, Votýpka J, Dostálová A *et al.* (2015) Infection Dynamics and Immune
1280 Response in a Newly Described *Drosophila*-Trypanosomatid Association. *mBio*, **6**,
1281 e01356–15.
1282 Handu M, Kaduskar B, Ravindranathan R *et al.* (2015) SUMO-Enriched Proteome for
1283 *Drosophila* Innate Immune Response. *G3*, **5**, 2137–2154.
1284 Harpur BA, Kent CF, Molodtsova D *et al.* (2014) Population genomics of the honey bee
1285 reveals strong signatures of positive selection on worker traits. *Proceedings of the*
1286 *National Academy of Sciences of the United States of America*, **111**, 2614–2619.
1287 Haselkorn TS, Markow TA, Moran NA (2009) Multiple introductions of the *Spiroplasma*
1288 bacterial endosymbiont into *Drosophila*. *Molecular Ecology*, **18**, 1294–1305.
1289 Hohenlohe PA, Bassham S, Etter PD *et al.* (2010) Population Genomics of Parallel
1290 Adaptation in Threespine Stickleback using Sequenced RAD Tags. *PLoS Genetics*, **6**,
1291 e1000862.
1292 Hu TT, Eisen MB, Thornton KR, Andolfatto P (2013) A second-generation assembly of the
1293 *Drosophila simulans* genome provides new insights into patterns of lineage-specific
1294 divergence. *Genome Research*, **23**, 89–98.
1295 Huang DW, Sherman BT, Lempicki RA (2009) Systematic and integrative analysis of large
1296 gene lists using DAVID bioinformatics resources. *Nature Protocols,* **4**, 44–57.

1297 Huang W, Massouras A, Inoue Y *et al.* (2014) Natural variation in genome architecture
1298 among 205 *Drosophila melanogaster* Genetic Reference Panel lines. *Genome*
1299 *Research*, **24**, 1193–1208.
1300 Hudson RR, Kreitman M, Aguadé M (1987) A test of neutral molecular evolution based on
1301 nucleotide data. *Genetics*, **116**, 153–159.
1302 Hutter S, Li H, Beisswanger S, De Lorenzo D, Stephan W (2007) Distinctly Different Sex
1303 Ratios in African and European Populations of *Drosophila melanogaster* Inferred From
1304 Chromosomewide Single Nucleotide Polymorphism Data. *Genetics*, **177**, 469–480.
1305 Jorde LB, Watkins WS, Bamshad MJ (2001) Population genomics: a bridge from
1306 evolutionary history to genetic medicine. *Human Molecular Genetics*, **10**, 2199–2207.
1307 Kao JY, Zubair A, Salomon MP, Nuzhdin SV, Campo D (2015) Population genomic
1308 analysis uncovers African and European admixture in *Drosophila melanogaster*
1309 populations from the south-eastern United States and Caribbean Islands. *Molecular*
1310 *Ecology*, **24**, 1499–1509.
1311 Kapopoulou A, Kapun M, Pavlidis P, *et al*. (2018a) Early split between African and
1312 European populations of *Drosophila melanogaster*. Preprint at *bioRxiv*, doi:
1313 https://doi.org/10.1101/340422
1314 Kapopoulou A, Pfeifer S, Jensen J, Laurent S (2018b). The demographic history of African
1315 *Drosophila melanogaster*. Preprint at *bioRxiv*, doi:10.1101/340406
1316 Kapitonov VV, Jurka J (2003) Molecular Paleontology of Transposable Elements in the
1317 *Drosophila melanogaster* Genome. *Proceedings of the National Academy of Sciences*
1318 *of the United States of America*, **100**, 6569–6574.
1319 Kapun M, Flatt T (2019) The adaptive significance of chromosomal inversion
1320 polymorphisms in *Drosophila melanogaster*. *Molecular Ecology*, **28**, 1263-1282

1321 Kapun M, Fabian DK, Goudet J, Flatt T (2016a) Genomic Evidence for Adaptive Inversion
1322 Clines in *Drosophila melanogaster*. *Molecular Biology and Evolution*, **33**, 1317–1336.
1323 Kapun M, Schmidt C, Durmaz E, Schmidt PS, Flatt T (2016b) Parallel effects of the
1324 inversion *In(3R)Payne* on body size across the North American and Australian clines in
1325 *Drosophila melanogaster. Journal of Evolutionary Biology*, **29**, 1059–1072.
1326 Kapun M, van Schalkwyk H, McAllister B, Flatt T, Schlötterer C (2014) Inference of
1327 chromosomal inversion dynamics from Pool-Seq data in natural and laboratory
1328 populations of *Drosophila melanogaster. Molecular Ecology*, **23**, 1813–1827.
1329 Kassis JA, Kennison JA, Tamkun JW (2017) Polycomb and Trithorax Group Genes in
1330 *Drosophila*. *Genetics*, **206**, 1699–1725.
1331 Kauer M, Zangerl B, Dieringer D, Schlötterer C (2002) Chromosomal patterns of
1332 microsatellite variability contrast sharply in African and non-African populations of
1333 *Drosophila melanogaster*. *Genetics*, **160**, 247–256.
1334 Keller A (2007) *Drosophila melanogaster*'s history as a human commensal. *Current*
1335 *Biology*, **17**, R77–R81.
1336 Kennington JW, Partridge L, Hoffmann AA (2006) Patterns of Diversity and Linkage
1337 Disequilibrium Within the Cosmopolitan Inversion *In(3R)Payne* in *Drosophila*
1338 *melanogaster* Are Indicative of Coadaptation. *Genetics*, **172**, 1655 – 1663.
1339 Kimura M (1984) *The Neutral Theory of Molecular Evolution*. Cambridge University Press.
1340 Knibb WR, Oakeshott JG, Gibson JB (1981) Chromosome Inversion Polymorphisms in
1341 *Drosophila melanogaster*. I. Latitudinal Clines and Associations between Inversions in
1342 Australasian Populations. *Genetics*, **98**, 833–847.
1343 Kofler R, Betancourt AJ, Schlötterer C (2012) Sequencing of pooled DNA samples (Pool-
1344 Seq) uncovers complex dynamics of transposable element insertions in *Drosophila*
1345 *melanogaster. PLoS Genetics*, **8**, e1002487.

1346 Kofler R, Orozco-terWengel P, De Maio N *et al.* (2011) PoPoolation: A Toolbox for
1347 Population Genetic Analysis of Next Generation Sequencing Data from Pooled
1348 Individuals. *PLoS ONE*, **6**, e15925.
1349 Kolaczkowski B, Hupalo DN, Kern AD (2011a) Recurrent adaptation in RNA interference
1350 genes across the *Drosophila* phylogeny. *Molecular Biology and Evolution*, **28**, 1033–
1351 1042.
1352 Kolaczkowski B, Kern AD, Holloway AK, Begun DJ (2011b) Genomic Differentiation
1353 Between Temperate and Tropical Australian Populations of *Drosophila melanogaster*.
1354 *Genetics*, **187**, 245–260.
1355 Korneliussen TS, Moltke I, Albrechtsen A, Nielsen R (2013) Calculation of Tajima's *D* and
1356 other neutrality test statistics from low depth next-generation sequencing data. *BMC*
1357 *Bioinformatics*, **14**, 289.
1358 Kreitman M (1983) Nucleotide polymorphism at the alcohol dehydrogenase locus of
1359 *Drosophila melanogaster*. *Nature*, **304**, 412–417.
1360 Kriesner P, Conner WR, Weeks AR, Turelli M, Hoffmann AA (2016) Persistence of a
1361 *Wolbachia* infection frequency cline in *Drosophila melanogaster* and the possible role
1362 of reproductive dormancy. *Evolution*, **70**, 979–997.
1363 Kühn I, Dormann CF (2012) Less than eight (and a half) misconceptions of spatial
1364 analysis. *Journal of Biogeography*, **39**, 995–998.
1365 Lachaise D, Cariou M-L, David JR *et al.* (1988) Historical Biogeography of the *Drosophila*
1366 *melanogaster* Species Subgroup. In Hecht MK, Wallace B, Prance GT (Eds.)
1367 *Evolutionary Biology* (pp. 159–225) Boston: Springer.
1368 Lack JB, Cardeno CM, Crepeau MW *et al.* (2015) The *Drosophila* genome nexus: a
1369 population genomic resource of 623 *Drosophila melanogaster* genomes, including 197
1370 from a single ancestral range population. *Genetics*, **199**, 1229–1241.

1371 Lack JB, Lange JD, Tang AD, Corbett-Detig RB, Pool JE (2016) A Thousand Fly
1372 Genomes: An Expanded *Drosophila* Genome Nexus. *Molecular Biology and Evolution*,
1373 **33**, 3308–3313.
1374 Lang DT (2014) *RJSONIO: Serialize R objects to JSON, JavaScript Object Notation*.
1375 https://CRAN.R-project.org/package=RJSONIO.
1376 Langley CH, Stevens K, Cardeno C *et al.* (2012) Genomic variation in natural populations
1377 of *Drosophila melanogaster*. *Genetics*, **192**, 533–598.
1378 Langmead B, Salzberg SL (2012) Fast gapped-read alignment with Bowtie 2. *Nature*
1379 *Methods*, **9**, 357–359.
1380 Larracuente AM, Roberts DM (2015) Genetics on the Fly: A Primer on the *Drosophila*
1381 Model System. *Genetics* **201**, 815–842.
1382 Lawrie DS, Messer PW, Hershberg R, Petrov DA (2013) Strong Purifying Selection at
1383 Synonymous Sites in *D. melanogaster*. *PLoS Genetics,* **9**, e1003527.
1384 Lerat E, Goubert C, Guirao-Rico S, Merenciano M, Dufour A-B, Vieira C, González J
1385 (2019) Population-specific dynamics and selection patterns of transposable element
1386 insertions in European natural populations. *Molecular Ecology*, **28**,1506–1522.
1387 Lemeunier F, Aulard S (1992). Inversion polymorphism in *Drosophila melanogaster.* In:
1388 Krimbas CB, & Powell JR (Eds.), *Drosophila Inversion Polymorphism* (pp. 339–405),
1389 New York: CRC Press.
1390 Lewontin RC (1974) *The Genetic Basis of Evolutionary Change*. Columbia University
1391 Press.
1392 Li H (2013) Aligning sequence reads, clone sequences and assembly contigs with BWA-
1393 MEM. Preprint at *arXiv.org*, 1303.3997
1394 Li H, Durbin R (2009) Fast and accurate short read alignment with Burrows-Wheeler
1395 transform. *Bioinformatics*, **25**, 1754–1760.

1396 Li H, Ruan J, Durbin R (2008) Mapping short DNA sequencing reads and calling variants
1397 using mapping quality scores. *Genome Research*, **18**, 1851–1858.
1398 Lian T, Li D, Tan X, Che T, Xu Z, Fan X, Wu N, Zhang L, Gaur U, Sun B, Yang M (2018)
1399 Genetic diversity and natural selection in wild fruit flies revealed by whole-genome
1400 resequencing. *Genomics,* **110**, 304–309.
1401 Luikart G, England PR, Tallmon D, Jordan S, Tableret P (2003) The power and promise of
1402 population genomics: from genotyping to genome typing. *Nature Reviews Genetics*, **4**,
1403 981–994.
1404 Lyne R, Smith R, Rutherford K *et al.* (2007) FlyMine: an integrated database for
1405 *Drosophila* and *Anopheles* genomics. *Genome Biology*, **8**, R129.
1406 Machado HE, Bergland AO, O'Brien KR *et al.* (2016) Comparative population genomics of
1407 latitudinal variation in *Drosophila simulans* and *Drosophila melanogaster*. *Molecular*
1408 *Ecology*, **25**, 723–740.
1409 Machado H, Bergland AO, Taylor R *et al.* (2018) Broad geographic sampling reveals
1410 predictable and pervasive seasonal adaptation in *Drosophila*. Preprint at *bioRxiv*, doi:
1411 https://doi.org/10.1101/337543.
1412 Mackay TFC, Richards S, Stone EA *et al.* (2012) The *Drosophila melanogaster* Genetic
1413 Reference Panel. *Nature*, **482**, 173–178.
1414 Martin M (2011) Cutadapt removes adapter sequences from high-throughput sequencing
1415 reads. *EMBnet.journal*, **17**, 10–12.
1416 Martino ME, Ma D, Leulier F (2017) Microbial influence on *Drosophila* biology. *Current*
1417 *Opinion in Microbiology*, **38**, 165–170.
1418 Mateo L, Rech GE, González J (2018) Genome-wide patterns of local adaptation in
1419 *Drosophila melanogaster*: adding intra European variability to the map. Preprint at
1420 *bioRxiv*, doi: https://doi.org/10.1101/269332

1421 Matthias P, Yoshida M, Khochbin S (2008) HDAC6 a new cellular stress surveillance
1422 factor. *Cell Cycle*, **7**, 7–10.
1423 McDonald JH, Kreitman M (1991) Adaptive protein evolution at the *Adh* locus in
1424 *Drosophila*. *Nature*, **351**, 652–654.
1425 McKenna A, Hanna M, Banks E *et al.* (2010) The Genome Analysis Toolkit: A MapReduce
1426 framework for analysing next-generation DNA sequencing data. *Genome Research*,
1427 **20**, 1297–1303.
1428 Menozzi P, Piazza A, Cavalli-Sforza L (1978) Synthetic maps of human gene frequencies
1429 in Europeans. *Science*, **201**, 786–792.
1430 Messer PW, Petrov DA (2013) Population genomics of rapid adaptation by soft selective
1431 sweeps. *Trends in Ecology & Evolution*, **28**, 659–669.
1432 Mettler LE, Voelker RA, Mukai T (1977) Inversion Clines in Populations of *Drosophila*
1433 *melanogaster. Genetics*, **87**, 169–176.
1434 Meyer F, Paarmann D, D'Souza M *et al.* (2008) The metagenomics RAST server - a public
1435 resource for the automatic phylogenetic and functional analysis of metagenomes. *BMC*
1436 *Bioinformatics*, **9**, 386.
1437 Micallef L, Rodgers P (2014) euler*APE*: drawing area-proportional 3-Venn diagrams using
1438 ellipses. *PLoS ONE*, **9**, e101717.
1439 Michalakis Y, Veuille M (1996) Length variation of CAG/CAA trinucleotide repeats in
1440 natural populations of *Drosophila melanogaster* and its relation to the recombination
1441 rate. *Genetics*, **143**, 1713–1725.
1442 Moran PAP (1950) Notes on Continuous Stochastic Phenomena. *Biometrika*, **37**, 17.
1443 Nei M (1987) *Molecular Evolutionary Genetics*. Columbia University Press.
1444 Nielsen R, Akey JM, Jakobsson M *et al.* (2017) Tracing the peopling of the world through
1445 genomics. *Nature*, **541**, 302-310.

1446 Nolte V, Pandey RV, Kofler R, Schlötterer C (2013) Genome-wide patterns of natural
1447 variation reveal strong selective sweeps and ongoing genomic conflict in *Drosophila*
1448 *mauritiana*. *Genome Research*, **23**, 99–110.
1449 Novembre J, Stephens M (2008) Interpreting principal component analyses of spatial
1450 population genetic variation. *Nature Genetics*, **40**, 646–649.
1451 Novembre J, Johnson T, Bryc K, *et al.* (2008) Genes mirror geography within Europe.
1452 *Nature*, **456**, 98-101.
1453 Nunes MDS, Neumeier H, Schlötterer C (2008) Contrasting patterns of natural variation in
1454 global *Drosophila melanogaster* populations. *Molecular Ecology*, **17**, 4470–4479.
1455 Okonechnikov K, Conesa A, García-Alcalde F (2016) Qualimap 2: advanced multi-sample
1456 quality control for high-throughput sequencing data. *Bioinformatics*, **32**, 292–294.
1457 Palmer WH, Medd NC, Beard PM, Obbard DJ (2018) Isolation of a natural DNA virus of
1458 Drosophila melanogaster, and characterisation of host resistance and immune
1459 responses. *PLOS Pathogens*, **14**, e1007050
1460 Parsch J, Novozhilov S, Saminadin-Peter SS, Wong KM, Andolfatto P (2010) On the utility
1461 of short intron sequences as a reference for the detection of positive and negative
1462 selection in *Drosophila*. *Molecular Biology and Evolution*, **27**, 1226–1234.
1463 Peel MC, Finlayson BL, McMahon TA (2007) Updated world map of the Köppen-Geiger
1464 climate classification. *Hydrology and Earth System Sciences*, **11**, 1633–1644.
1465 Petrov DA, Fiston-Lavier AS, Lipatov M, Lenkov K, González J (2011) Population
1466 Genomics of Transposable Elements in *Drosophila melanogaster*. *Molecular Biology*
1467 *and Evolution*, **28**, 1633–1644.
1468 Pool JE (2015) The Mosaic Ancestry of the *Drosophila* Genetic Reference Panel and the
1469 *D. melanogaster* Reference Genome Reveals a Network of Epistatic Fitness
1470 Interactions. *Molecular Biology and Evolution*, **32**, 3236–3251.

1471 Pool JE, Nielsen R (2007) Population size changes reshape genomic patterns of diversity.
1472 *Evolution*, **61**, 3001–3006.
1473 Pool JE, Braun DT, Lack JB (2016) Parallel Evolution of Cold Tolerance Within *Drosophila*
1474 *melanogaster*. *Molecular Biology and Evolution*, **34,** 349–360.
1475 Pool JE, Corbett-Detig RB, Sugino RP *et al.* (2012) Population Genomics of Sub-Saharan
1476 *Drosophila melanogaster*: African Diversity and Non-African Admixture. *PLoS*
1477 *Genetics*, **8**, e1003080.
1478 Powell JR (1997) *Progress and Prospects in Evolutionary Biology: The Drosophila Model*.
1479 Oxford University Press.
1480 R Development Core Team (2009) R: A Language and Environment for Statistical
1481 Computing. *R-project.org*.
1482 Rako L, Anderson AR, Sgrò CM, Stocker AJ, Hoffmann AA (2006) The association
1483 between inversion *In(3R)Payne* and clinally varying traits in *Drosophila melanogaster.*
1484 *Genetica*, **128**, 373–384.
1485 Rane RV, Rako L, Kapun M, LEE SF (2015) Genomic evidence for role of inversion *3RP*
1486 of *Drosophila melanogaster* in facilitating climate change adaptation. *Molecular*
1487 *Ecology*, **24**, 2423–2432.
1488 Rech GE, Bogaerts-Márquez M, Barrón MG, Merenciano M, Villanueva-Cañas JL, Horváth
1489 V, Fiston-Lavier A-S, Luyten I, Venkataram S, Quesneville H, Petrov DA, González J
1490 (2019) Stress response, behavior, and development are shaped by transposable
1491 element-induced mutations in *Drosophila*. *PLOS Genetics,* **15**, e1007900.
1492 Reinhardt JA, Kolaczkowski B, Jones CD, Begun DJ, Kern AD (2014) Parallel Geographic
1493 Variation in *Drosophila melanogaster*. *Genetics*, **197**, 361–373.
1494 Richardson MF, Weinert LA, Welch JJ *et al.* (2012) Population Genomics of the *Wolbachia*
1495 Endosymbiont in *Drosophila melanogaster. PLoS Genetics*, **8**, e1003129.

1496 Rogers RL, Hartl DL (2012) Chimeric genes as a source of rapid evolution in *Drosophila*
1497 *melanogaster*. *Molecular Biology and Evolution*, **29**, 517–529.
1498 Rozas J, Ferrer-Mata A, Sánchez-DelBarrio JC *et al.* (2017) DnaSP 6: DNA Sequence
1499 Polymorphism Analysis of Large Datasets. *Molecular Biology and Evolution*, **34**, 3299–
1500 3302.
1501 Salmela L, Schröder J (2011) Correcting errors in short reads by multiple alignments.
1502 *Bioinformatics*, **27**, 1455–1461.
1503 Schlenke TA, Begun DJ (2003) Natural selection drives *Drosophila* immune system
1504 evolution. *Genetics*, **164**, 1471–1480.
1505 Schlötterer C, Neumeier H, Sousa C, Nolte V (2006) Highly structured Asian *Drosophila*
1506 *melanogaster* populations: a new tool for hitchhiking mapping? *Genetics*, **172**, 287–
1507 292.
1508 Schlötterer C, Tobler R, Kofler R, Nolte V (2014) Sequencing pools of individuals - mining
1509 genome-wide polymorphism data without big funding. *Nature Reviews Genetics*, **15**,
1510 749–763.
1511 Schmidt JM, Good RT, Appleton B *et al.* (2010) Copy number variation and transposable
1512 elements feature in recent, ongoing adaptation at the *Cyp6g1* locus. *PLoS Genetics*, **6**,
1513 e1000998.
1514 Schmidt PS, Paaby AB (2008) Reproductive Diapause and Life-History Clines in North
1515 American Populations of *Drosophila melanogaster*. *Evolution*, **62**, 1204–1215.
1516 Schmidt PS, Zhu CT, Das J *et al.* (2008) An amino acid polymorphism in the *couch potato*
1517 gene forms the basis for climatic adaptation in *Drosophila melanogaster*. *Proceedings*
1518 *of the National Academy of Sciences of the United States of America*, **105**, 16207–
1519 16211.

1520 Sella G, Petrov DA, Przeworski M, Andolfatto P (2009) Pervasive Natural Selection in the
1521 *Drosophila* Genome? *PLoS Genetics*, **5**, e1000495.
1522 Singh ND, Arndt PF, Clark AG, Aquadro CF (2009) Strong evidence for lineage and
1523 sequence specificity of substitution rates and patterns in *Drosophila*. *Molecular Biology*
1524 *and Evolution*, **26**, 1591–1605.
1525 Slatkin M. 1985. Gene Flow in Natural Populations. *Annual Review of Ecology and*
1526 *Systematics* **16**:393–430.
1527 Staubach F, Baines JF, Künzel S, Bik EM, Petrov DA (2013) Host species and
1528 environmental effects on bacterial communities associated with *Drosophila* in the
1529 laboratory and in the natural environment. *PLoS ONE*, **8**, e70749.
1530 Stephan W (2010) Genetic hitchhiking versus background selection: the controversy and
1531 its implications. *Philosophical Transactions of the Royal Society of London B*, **365**,
1532 1245–1253.
1533 Tajima F (1989) Statistical method for testing the neutral mutation hypothesis by DNA
1534 polymorphism. *Genetics*, **123**, 585–595.
1535 Tajima F (1983) Evolutionary relationship of DNA sequences in finite populations.
1536 *Genetics* **105**, 437–460.
1537 Thurmond J, Goodman JL, Strelets VB, Attrill H, Gramates LS, Marygold SJ, Matthews
1538 BB, Millburn G, Antonazzo G, Trovisco V, Kaufman TC, Calvi BR, FlyBase Consortium
1539 (2019) FlyBase 2.0: the next generation. *Nucleic Acids Res,* **47**, D759–D765.
1540 Trinder M, Daisley BA, Dube JS, Reid G (2017) *Drosophila melanogaster* as a High-
1541 Throughput Model for Host-Microbiota Interactions. *Frontiers in Microbiology*, **8**, 751.
1542 Turner TL, Levine MT, Eckert ML, Begun DJ (2008) Genomic analysis of adaptive
1543 differentiation in *Drosophila melanogaster*. *Genetics*, **179**, 455–473.

1544 Umina PA, Weeks AR, Kearney MR, McKechnie SW, Hoffmann AA (2005) A rapid shift in
1545 a classic clinal pattern in *Drosophila* reflecting climate change. *Science*, **308**, 691–693.
1546 Unckless RL (2011) A DNA virus of *Drosophila*. *PLoS ONE*, **6**, e26564.
1547 Walters AM, Matthews MK, Hughes R, Malcolm Jaanna, Rudman S, Newell PD, Douglas
1548 AE, Schmidt PS, Chaston JM (2018) The microbiota influences the Drosophila
1549 melanogaster life history strategy. bioRxiv. 471540
1550 Wang Y, Kapun M, Waidele L, Kuenzel S, Bergland AO, Staubach F (2019) Continent-
1551 wide structure of bacterial microbiomes of European Drosophila melanogaster
1552 suggests host-control. bioRxiv. 527531
1553 Wang Y, Staubach F (2018); Individual variation of natural *D.melanogaster*-associated
1554 bacterial communities, *FEMS Microbiology Letters*, **365**, fny017
1555 Watterson GA (1975) On the number of segregating sites in genetical models without
1556 recombination. *Theoretical Population Biology*, **7**, 256–276.
1557 Webster CL, Longdon B, Lewis SH, Obbard DJ (2016) Twenty-Five New Viruses
1558 Associated with the Drosophilidae (Diptera). *Evolutionary Bioinformatics Online*, **12**,
1559 13–25.
1560 Webster CL, Waldron FM, Robertson S *et al.* (2015) The Discovery, Distribution, and
1561 Evolution of Viruses Associated with *Drosophila melanogaster. PLoS Biology*, **13**,
1562 e1002210.
1563 Weir BS, Cockerham CC (1984) Estimating *F*-Statistics for the Analysis of Population
1564 Structure. *Evolution*, **38**, 1358–1370.
1565 Werren JH, Baldo L, Clark ME (2008) Wolbachia: master manipulators of invertebrate
1566 biology. *Nature Reviews Microbiology*, **6**, 741–751.
1567 Wickham H (2016) *ggplot2: Elegant Graphics for Data Analysis*. Springer.

1568 Wilfert L, Longdon B, Ferreira AGA, Bayer F, Jiggins FM (2011) Trypanosomatids are
1569 common and diverse parasites of *Drosophila*. *Parasitology*, **138**, 858–865.
1570 Wolf JBW, Bayer T, Haubold B *et al.* (2010) Nucleotide divergence vs. gene expression
1571 differentiation: comparative transcriptome sequencing in natural isolates from the
1572 carrion crow and its hybrid zone with the hooded crow. *Molecular Ecology*, **19**, 162–
1573 175.
1574 Wolff JN, Camus MF, Clancy DJ, Dowling DK (2016) Complete mitochondrial genome
1575 sequences of thirteen globally sourced strains of fruit fly (*Drosophila melanogaster*)
1576 form a powerful model for mitochondrial research. *Mitochondrial DNA Part A,* **27**,
1577 4672–4674.
1578 Xiao F-X, Yotova V, Zietkiewicz E *et al.* (2004) Human *X*-chromosomal lineages in Europe
1579 reveal Middle Eastern and Asiatic contacts. *European Journal of Human Genetics*, **12**,
1580 301–311.
1581 Yukilevich R, True JR (2008a) Incipient sexual isolation among cosmopolitan *Drosophila*
1582 *melanogaster* populations. *Evolution*, **62**, 2112–2121.
1583 Yukilevich R, True JR (2008b) African morphology, behavior and phermones underlie
1584 incipient sexual isolation between us and Caribbean *Drosophila melanogaster.*
1585 *Evolution*, **62**, 2807–2828.
1586 Yukilevich R, Turner TL, Aoki F, Nuzhdin SV, True JR (2010) Patterns and processes of
1587 genome-wide divergence between North American and African *Drosophila*
1588 *melanogaster*. *Genetics*, **186**, 219–239.
1589 Zanini F, Brodin J, Thebo L *et al.* (2015) Population genomics of intrapatient HIV-1
1590 evolution. *eLife*, **4**, e11282.
1591

## Tables

**Table 1. Sample information for all populations in the *DrosEU* dataset.** Origin, collection date, season and sample size (number of chromosomes: *n*) of the 48 samples in the *DrosEU* 2014 data set. Additional information can be found in Table S1.

| ID | Country | Location | Coll. Date | Number ID | Lat (°) | Lon (°) | Alt (m) | Season | n | Coll. name |
|---|---|---|---|---|---|---|---|---|---|---|
| AT_Mau_14_01 | Austria | Mauternbach | 2014-07-20 | 1 | 48.38 | 15.56 | 572 | S | 80 | Andrea J. Betancourt |
| AT_Mau_14_02 | Austria | Mauternbach | 2014-10-19 | 2 | 48.38 | 15.56 | 572 | F | 80 | Andrea J. Betancourt |
| TR_Yes_14_03 | Turkey | Yesiloz | 2014-08-31 | 3 | 40.23 | 32.26 | 680 | S | 80 | Banu Sebnem Onder |
| TR_Yes_14_04 | Turkey | Yesiloz | 2014-10-23 | 4 | 40.23 | 32.26 | 680 | F | 80 | Banu Sebnem Onder |
| FR_Vil_14_05 | France | Viltain | 2014-08-18 | 5 | 48.75 | 2.16 | 153 | S | 80 | Catherine Montchamp-Moreau |
| FR_Vil_14_07 | France | Viltain | 2014-10-27 | 7 | 48.75 | 2.16 | 153 | F | 80 | Catherine Montchamp-Moreau |
| FR_Got_14_08 | France | Gotheron | 2014-07-08 | 8 | 44.98 | 4.93 | 181 | S | 80 | Cristina Vieira |
| UK_She_14_09 | United Kingdom | Sheffield | 2014-08-25 | 9 | 53.39 | -1.52 | 100 | S | 80 | Damiano Porcelli |
| UK_Sou_14_10 | United Kingdom | South Queensferry | 2014-07-14 | 10 | 55.97 | -3.35 | 19 | S | 80 | Darren Obbard |
| CY_Nic_14_11 | Cyprus | Nicosia | 2014-08-10 | 11 | 35.07 | 33.32 | 263 | S | 80 | Eliza Argyridou |
| UK_Mar_14_12 | United Kingdom | Market Harborough | 2014-10-20 | 12 | 52.48 | -0.92 | 80 | F | 80 | Eran Tauber |
| UK_Lut_14_13 | United Kingdom | Lutterworth | 2014-10-20 | 13 | 52.43 | -1.10 | 126 | F | 80 | Eran Tauber |

| | | | | | | | | | | |
|---|---|---|---|---|---|---|---|---|---|---|
| DE_Bro_14_14 | Germany | Broggingen | 2014-06-26 | 14 | 48.22 | 7.82 | 173 | S | 80 | Fabian Staubach |
| DE_Bro_14_15 | Germany | Broggingen | 2014-10-15 | 15 | 48.22 | 7.82 | 173 | F | 80 | Fabian Staubach |
| UA_Yal_14_16 | Ukraine | Yalta | 2014-06-20 | 16 | 44.50 | 34.17 | 72 | S | 80 | Iryna Kozeretska |
| UA_Yal_14_18 | Ukraine | Yalta | 2014-08-27 | 18 | 44.50 | 34.17 | 72 | S | 80 | Iryna Kozeretska |
| UA_Ode_14_19 | Ukraine | Odesa | 2014-07-03 | 19 | 46.44 | 30.77 | 54 | S | 80 | Iryna Kozeretska |
| UA_Ode_14_20 | Ukraine | Odesa | 2014-07-22 | 20 | 46.44 | 30.77 | 54 | S | 80 | Iryna Kozeretska |
| UA_Ode_14_21 | Ukraine | Odesa | 2014-08-29 | 21 | 46.44 | 30.77 | 54 | S | 80 | Iryna Kozeretska |
| UA_Ode_14_22 | Ukraine | Odesa | 2014-10-10 | 22 | 46.44 | 30.77 | 54 | F | 80 | Iryna Kozeretska |
| UA_Kyi_14_23 | Ukraine | Kyiv | 2014-08-09 | 23 | 50.34 | 30.49 | 179 | S | 80 | Iryna Kozeretska |
| UA_Kyi_14_24 | Ukraine | Kyiv | 2014-09-08 | 24 | 50.34 | 30.49 | 179 | F | 80 | Iryna Kozeretska |
| UA_Var_14_25 | Ukraine | Varva | 2014-08-18 | 25 | 50.48 | 32.71 | 125 | S | 80 | Oleksandra Protsenko |
| UA_Pyr_14_26 | Ukraine | Pyriatyn | 2014-08-20 | 26 | 50.25 | 32.52 | 114 | S | 80 | Oleksandra Protsenko |
| UA_Dro_14_27 | Ukraine | Drogobych | 2014-08-24 | 27 | 49.33 | 23.50 | 275 | S | 80 | Iryna Kozeretska |
| UA_Cho_14_28 | Ukraine | Chornobyl | 2014-09-13 | 28 | 51.37 | 30.14 | 121 | F | 80 | Iryna Kozeretska |
| UA_Cho_14_29 | Ukraine | Chornobyl Yaniv | 2014-09-13 | 29 | 51.39 | 30.07 | 121 | F | 80 | Iryna Kozeretska |
| SE_Lun_14_30 | Sweden | Lund | 2014-07-31 | 30 | 55.69 | 13.20 | 51 | S | 80 | Jessica Abbott |
| DE_Mun_14_31 | Germany | Munich | 2014-06-19 | 31 | 48.18 | 11.61 | 520 | S | 80 | John Parsch |
| DE_Mun_14_32 | Germany | Munich | 2014-09-03 | 32 | 48.18 | 11.61 | 520 | F | 80 | John Parsch |
| PT_Rec_14_33 | Portugal | Recarei | 2014-09-26 | 33 | 41.15 | -8.41 | 175 | F | 80 | Jorge Vieira |

| | | | | | | | | | | |
|---|---|---|---|---|---|---|---|---|---|---|
| ES_Gim_14_34 | Spain | Gimenells (Lleida) | 2014-10-20 | 34 | 41.62 | 0.62 | 173 | F | 80 | Lain Guio |
| ES_Gim_14_35 | Spain | Gimenells (Lleida) | 2014-08-13 | 35 | 41.62 | 0.62 | 173 | S | 80 | Lain Guio |
| FI_Aka_14_36 | Finland | Akaa | 2014-07-25 | 36 | 61.10 | 23.52 | 88 | S | 80 | Maaria Kankare |
| FI_Aka_14_37 | Finland | Akaa | 2014-08-27 | 37 | 61.10 | 23.52 | 88 | S | 80 | Maaria Kankare |
| FI_Ves_14_38 | Finland | Vesanto | 2014-07-26 | 38 | 62.55 | 26.24 | 121 | S | 66 | Maaria Kankare |
| DK_Kar_14_39 | Denmark | Karensminde | 2014-09-01 | 39 | 55.95 | 10.21 | 15 | F | 80 | Mads Fristrup Schou |
| DK_Kar_14_41 | Denmark | Karensminde | 2014-11-25 | 41 | 55.95 | 10.21 | 15 | F | 80 | Mads Fristrup Schou |
| CH_Cha_14_42 | Switzerland | Chalet à Gobet | 2014-07-24 | 42 | 46.57 | 6.70 | 872 | S | 80 | Martin Kapun |
| CH_Cha_14_43 | Switzerland | Chalet à Gobet | 2014-10-05 | 43 | 46.57 | 6.70 | 872 | F | 80 | Martin Kapun |
| AT_See_14_44 | Austria | Seeboden | 2014-08-17 | 44 | 46.81 | 13.51 | 591 | S | 80 | Martin Kapun |
| UA_Kha_14_45 | Ukraine | Kharkiv | 2014-07-26 | 45 | 49.82 | 36.05 | 141 | S | 80 | Svitlana Serga |
| UA_Kha_14_46 | Ukraine | Kharkiv | 2014-09-14 | 46 | 49.82 | 36.05 | 141 | F | 80 | Svitlana Serga |
| UA_Cho_14_47 | Ukraine | Chornobyl Applegarden | 2014-09-13 | 47 | 51.27 | 30.22 | 121 | F | 80 | Svitlana Serga |
| UA_Cho_14_48 | Ukraine | Chornobyl Polisske | 2014-09-13 | 48 | 51.28 | 29.39 | 121 | F | 70 | Svitlana Serga |
| UA_Kyi_14_49 | Ukraine | Kyiv | 2014-10-11 | 49 | 50.34 | 30.49 | 179 | F | 80 | Svitlana Serga |
| UA_Uma_14_50 | Ukraine | Uman | 2014-10-01 | 50 | 48.75 | 30.21 | 214 | F | 80 | Svitlana Serga |
| RU_Val_14_51 | Russia | Valday | 2014-08-17 | 51 | 57.98 | 33.24 | 217 | S | 80 | Elena Pasyukova |

1595

**Table 2**. **Clinality of genetic variation and population structure.** Effects of geographic variables and/or seasonality on genome-wide average levels of diversity ($\pi$, $\theta$ and Tajima's $D$; top rows) and on the first three axes of a PCA based on allele frequencies at neutrally evolving sites (bottom rows). The values represent $F$-ratios from general linear models. Bold type indicates $F$-ratios that are significant after Bonferroni correction (adjusted $\alpha'$=0.0055). Asterisks in parentheses indicate significance when accounting for spatial autocorrelation by spatial error models. These models were only calculated when Moran's $I$ test, as shown in the last column, was significant. *$p$ < 0.05; **$p$ < 0.01; ***$p$ < 0.001.

| ***Factor*** | ***Latitude*** | ***Longitude*** | ***Altitude*** | ***Season*** | ***Moran's I*** |
|---|---|---|---|---|---|
| $\pi_{(X)}$ | 4.11* | 1.62 | **15.23*** ** | 1.65 | 0.86 |
| $\pi_{(Aut)}$ | 0.91 | 2.54 | **27.18*** ** | 0.16 | -0.86 |
| $\theta_{(X)}$ | 2.65 | 1.31 | **15.54*** ** | 2.22 | 0.24 |
| $\theta_{(Aut)}$ | 0.48 | 1.44 | **13.66*** ** | 0.37 | -1.13 |
| $D_{(X)}$ | 0.02 | 0.38 | 5.93* | 3.26 | -2.08 |
| $D_{(Aut)}$ | 0.09 | 0.76 | 5.33* | 0.71 | -1.45 |
| PC1 | 0.06 | **120.72*** (***)** | 5.35*(*) | 2.53 | 4.15*** |
| PC2 | 3.5 | **10.22** ** | **15.21*** ** | 1.97 | -1.96 |
| PC3 | 0.14 | 0.11 | 0.01 | 1.29 | 0.22 |

**Table 3**. **Clinality and/or seasonality of chromosomal inversions.** The values represent *F*-ratios from generalized linear models with a binomial error structure to account for frequency data. Bold type indicates deviance values that were significant after Bonferroni correction (adjusted *α'*=0.0071). Stars in parentheses indicate significance when accounting for spatial autocorrelation by spatial error models. These models were only calculated when Moran's *I* test, as shown in the last column, was significant. *$p < 0.05$; **$p < 0.01$; ***$p < 0.001$

| ***Factor*** | ***Latitude*** | ***Longitude*** | ***Altitude*** | ***Season*** | ***Moran's I*** |
|---|---|---|---|---|---|
| *In(2L)t* | 2.2 | **10.09**** | **43.94***** | 0.89 | -0.92 |
| *In(2R)NS* | 0.25 | **14.43***** | 2.88 | 2.43 | 1.25 |
| *In(3L)P* | **21.78***** | 2.82 | 0.62 | 3.6 | -1.61 |
| *In(3R)C* | **18.5***(***)** | 0.75 | 1.42 | 0.04 | 2.79** |
| *In(3R)Mo* | 0.3 | 0.09 | 0.35 | 0.03 | -0.9 |
| *In(3R)Payne* | **43.47***** | 0.66 | 1.69 | 1.55 | -0.89 |

## Supplementary Files

Supplementary File 1. Supplementary Tables.

This file contains the 13 supplementary tables mention in the text.

Supplementary File 2. Additional methods.

This file contains the additional methods mention in the text.